

PLATELET FACTOR 4 INTERACTION WITH ADENOVIRAL VACCINES

EVALUATING THE INTERACTION OF PLATELET FACTOR 4
AND ADENOVIRAL VECTOR-BASED SARS-COV-2 VACCINES
IN THE PATHOGENESIS OF
VACCINE-INDUCED IMMUNE THROMBOTIC THROMBOCYTOPENIA

By: YI ZHANG, B.Sc. (Hon.)

A Thesis

Submitted to the School of Graduate Studies in

Partial Fulfilment of the Requirements for the Degree

Master of Science

McMaster University

© Copyright Yi Zhang, August 2024

M.Sc Thesis – Y. Zhang; McMaster University – Biochemistry

MASTER OF SCIENCE (2024)

McMaster University

(Biochemistry and Biomedical Sciences)

Hamilton, Ontario

TITLE: Evaluating the Interaction of Platelet Factor 4 and Adenoviral Vector Based
COVID-19 Vaccines in the Pathogenesis of Vaccine-induced Immune Thrombotic
Thrombocytopenia

AUTHOR: Yi Zhang, B.Sc. (Hon.) (University of Waterloo)

SUPERVISOR: Dr. Ishac Nazy

SUPERVISORY COMMITTEE: Dr. Donald Arnold, Dr. Sara Andres, Dr. Zhou
Xing

NUMBER OF PAGES: xvii, 92

LAY ABSTRACT

This study investigates how adenoviral vector (AdV)-based COVID-19 vaccines cause vaccine-induced immune thrombotic thrombocytopenia (VITT), a side effect involving the development of antibodies against platelet factor 4 (PF4), resulting in blood clots and low platelet counts. We focus on PF4 interaction with the vaccines and the role of inflammation-related cytokines in potentially correlating with VITT disease severity and anti-PF4 antibody formation.

The PF4/vaccine interactions were only detected using the higher sensitivity technology of surface plasmon resonance and could not be confirmed with biolayer interferometry, indicating weak interactions between PF4 and the vaccines. Severe VITT patients exhibited elevated levels of inflammatory cytokine, linking an elevated inflammatory state to disease severity. Additionally, heparin-induced thrombocytopenia (HIT) patients, who exhibit pathogenic anti-PF4 antibodies and share similar clinical features with VITT, displayed even higher inflammatory cytokine levels, suggesting that the development and activity of VITT and HIT antibodies may be associated with distinct cytokine environments.

ABSTRACT

The widespread use of adenoviral (AdV)-based SARS-CoV-2 vaccines, such as ChAdOx1-S (AstraZeneca) and Ad26.COV2.S (Johnson & Johnson/Janssen), has been crucial in combating the COVID-19 pandemic. However, these vaccines have been linked to vaccine-induced immune thrombotic thrombocytopenia (VITT), characterized by the formation of anti-platelet factor 4 (PF4) antibodies, leading to thrombosis and thrombocytopenia.

Previous research has demonstrated that PF4 bound to polyanionic heparin forms immunogenic complexes, resulting in anti-PF4 antibody development in heparin-induced thrombocytopenia. Similar mechanisms have been proposed for VITT, where polyanionic AdV bound to PF4 triggers antibody development. However, inconsistent findings regarding PF4/vaccine interactions necessitate further exploration of factors, such as inflammatory cytokines, that may support antibody development.

This study verifies the interactions between PF4 and AdV-based vaccines while analyzing the VITT cytokine profiles. Our aim is to understand whether PF4 and AdV-based vaccines have the potential to form immunogenic complexes and the role of a heightened inflammatory environment, potentially associated with anti-PF4 antibody formation and disease severity.

While significant interactions between PF4 and both vaccines were detected using surface plasmon resonance (SPR), these interactions could not be confirmed using biolayer interferometry. Since SPR exhibits higher sensitivity, this discrepancy suggests a weak interaction between PF4 and the vaccines. Cytokine analysis revealed that VITT patients with CVST exhibited elevated interleukin-8

levels, linking disease severity to a heightened inflammatory state. Additionally, HIT patients displayed even higher levels of inflammatory cytokines, which may be attributed to HIT antibody-related mechanisms or their pre-existing health conditions.

In conclusion, there is a weak interaction between PF4 and the vaccines. Additional research is needed to determine if this complex can function as an immunogen under physiological conditions. Moreover, while an elevated inflammatory state is linked to VITT severity, the development and activity of VITT and HIT antibodies may be associated with distinct cytokine environments.

ACKNOWLEDGEMENTS

I would like to express my deepest gratitude to everyone who have accompanied me through my MSc journey. This work would not have been possible without your help, support, and inspiration.

I am truly grateful to my supervisor, Dr. Ishac Nazy, for his constant support and guidance. Your unwavering enthusiasm have always driven me to keep reaching for my goals. I would also like to extend my gratitude to my committee members and supervisors: Dr. Sara Andres, Dr. Zhou Xing, Dr. Donald Arnold, and Dr. John Kelton. Your encouragement, valuable expertise, and insightful feedback have been instrumental in shaping my research and academic growth.

Special thanks to Dr. James Fredenburgh and the members of Dr. Jeffery Weitz's lab at TaARI for welcoming me into their lab, treating me as one of their own, and calling me their adopted student. Your acceptance and support have brightened my day every time I visited TaARI.

To all the past and present members of the Platelet Immunology Lab, this thesis would not have been possible without you. Thank you for creating a collaborative, supportive, and encouraging environment. Your company and constant willingness to help have been therapeutic during the challenging times of my thesis writing.

To my benchmate, Dr. Nikolas Ivetic, thank you for your knowledgeable advice and for sharing the pessimistic moments with me. To Michael Hack, your constant

smile and positive energy always manage to brighten up the day. To Jared Treverton, your continuous inspiration has been invaluable for my project. To Rumi Clare and Hina Bhakta, thank you for always being patient and willing to help with any problems or questions that come your way.

I am also grateful for the therapy sessions and midnight science talks with Anna-Lise Bissola, Michael Hack, and Jared Treverton. You all have a unique ability to boost my motivations and reignite my passion for science.

To my bestie, Chen Niu, whom I found through the lab, you have truly been like a long-lost sister to me. Your company and your dramatic flair always have a way of making life more interesting and brighten even the toughest moments.

Finally, I would like to express my deepest gratitude for the unconditional love and support from my family and friends. Thank you for enduring my emotional ups and downs and for being my unwavering source of encouragement. To my mom and dad, who sacrificed everything to relocate to a foreign country to provide me with better education and opportunities: Thank you for standing by my side, supporting my decisions, and loving me despite my imperfections.

Once again, thank you so much for being there through the good times and the bad.

TABLE OF CONTENTS

TITLE PAGE	I
DESCRIPTIVE NOTE	II
LAY ABSTRACT	III
ABSTRACT	IV
ACKNOWLEDGEMENTS	VI
TABLE OF CONTENTS	VIII
LIST OF FIGURES	XI
LIST OF TABLES	XII
LIST OF SUPPLEMENTARY FIGURES	XIII
LIST OF SUPPLEMENTARY TABLES	XIV
LIST OF ABBREVIATIONS	XV
DECLARATION OF ACADEMIC ACHIEVEMENT	XVII
1.0 INTRODUCTION	1
1.1 COVID-19 pandemic and vaccination efforts	1
1.2 Adverse events associated with SARS-CoV-2 vaccination.	1
1.3 Adverse effects following Adenoviral vector (AdV)-based vaccine administration.....	2
1.4 AdV-based vaccines	5
1.5 Heparin-induced thrombocytopenia (HIT)	6
1.6 Vaccine-induced immune thrombosis and thrombocytopenia (VITT)	10
1.6.1 <i>Clinical and laboratory features of VITT</i>	10
1.6.2 <i>Characteristics of VITT anti-platelet factor 4 (PF4) antibodies</i>	11
1.6.3 <i>Proposed pathogenic mechanisms of VITT and conflicting findings...</i>	12
1.7 Cytokine involvement in thrombotic disorders.....	15
1.7.1 <i>Implication of proinflammatory cytokines in venous thrombosis</i>	16
1.7.2 <i>Cytokine involvement in B-cell activation and antibodies development</i>	18
2.0. RESEARCH OUTLINE	19
2.1. Aim.....	19
2.2. Rationale	20
2.3. Hypothesis.....	21

2.4. Objectives.....	21
3.0 MATERIALS AND METHODS.....	23
3.1 Interaction analysis	23
3.1.1 <i>BLI interaction assays</i>	23
3.1.2 <i>SPR interaction assays</i>	25
3.1.3 <i>Data acquisition and statistical analysis</i>	26
3.2 Cytokine profiling.....	28
3.2.1 <i>Study design</i>	28
3.2.2 <i>Patient population</i>	28
3.2.3 <i>Cytokine level testing</i>	29
3.2.4 <i>Statistical analysis</i>	29
4.0 RESULTS.....	30
4.1 Interaction analysis of AdV-based vaccines and PF4	30
4.1.1 <i>Biolayer interferometry (BLI)</i>	30
4.1.2 <i>Surface plasmon resonance (SPR)</i>	31
4.2 Cytokine profiling.....	34
4.2.1 <i>No significant association between cytokine levels and VITT antibodies development</i>	34
4.2.2 <i>HIT patients exhibit an elevated inflammatory state compared to VITT patients</i>	34
4.2.3 <i>VITT disease severity correlates with a heightened inflammatory state</i>	35
5.0 DISCUSSION	36
5.1 Interaction analysis between PF4 and AdV-based vaccines	38
5.1.1 <i>BLI is unsuitable for illustrating reversible binding between PF4 and AdV-based vaccines</i>	38
5.1.2 <i>SPR demonstrated binding only between PF4 and the Ad26-based vaccines when bPF4 acts as the ligand</i>	41
5.1.3 <i>SPR demonstrated binding between PF4 and all three vaccines when PF4 is used as the analyte</i>	43
5.1.3 <i>Limitations</i>	48
5.2 Cytokine profiling of VITT patients	48
5.2.1 <i>No significant correlations found between cytokine levels and antibody production in VITT</i>	48
5.2.2 <i>VITT and HIT anti-PF4 antibodies are associated with distinct cytokine profiles</i>	53

5.2.3 <i>VITT patients with CVST exhibit higher levels of IL-8 compared to those without CVST</i>	57
5.2.4 <i>Limitations</i>	59
6.0 CONCLUSIONS	60
8.0 FIGURES	63
9.0 TABLES	72
10.0 SUPPLEMENTARY FIGURES	73
11.0 SUPPLEMENTARY TABLES	78
12.0 BIBLIOGRAPHY	84

LIST OF FIGURES

Figure 1. BLI interaction analysis of AdV-based vaccines with immobilized bPF4 using streptavidin sensors.

Figure 2. BLI control experiments with immobilized bPF4 using streptavidin sensors.

Figure 3. BLI interaction analysis of PF4 with immobilized Adv-based vaccines using amine coupling sensors.

Figure 4. SPR interaction analysis of Adv-based vaccines and immobilized bPF4 using streptavidin-coated CM4 sensors.

Figure 5. SPR control experiments with immobilized bPF4 using streptavidin-coated CM4 sensors.

Figure 6. SPR interaction analysis of PF4 and immobilized AdV-based vaccines using anti-hexon coated amine coupling C1 sensors.

Figure 7. SPR control experiments with PF4 in the flow phase using amine coupling C1 sensors.

Figure 8. Cytokine level distributions in sera of VITTpos patient with and without CVST.

Figure 9. Cytokine level distributions of VITTpos and VITTneg patients.

Figure 10. Cytokine level distributions of VITTpos and HITpos patients relative to their respective reference.

LIST OF TABLES

Table 1. Cytokine profiling patient characteristics.

LIST OF SUPPLEMENTARY FIGURES

Supplementary Figure 1. Background interaction of ChAdOx1-S to streptavidin-coated reference cell using CM4 sensors in SPR.

Supplementary Figure 2. Background interaction of Ad26.COVS2.S to streptavidin-coated reference cell using CM4 sensors in SPR.

Supplementary Figure 3. Background interaction of Ad26.ZIKV to streptavidin-coated reference cell using CM4 sensors in SPR.

Supplementary Figure 4. BLI interaction analysis of anti-hexon detection of ChAdOx1-S captured on amine-coupled sensors.

Supplementary Figure 5. Amine coupling reaction mechanism.

LIST OF SUPPLEMENTARY TABLES

Supplementary Table 1. Comparison of serum cytokine levels in fluorescence intensity of suspected VITT patients with and without anti-PF4 antibodies during the acute phase.

Supplementary Table 2. Comparison of serum cytokine levels in fluorescence intensity of VITT and HIT patients.

Supplementary Table 3. Serum cytokine levels in fluorescence intensity of VITT patients with CVST compared to those with thrombosis in other sites during the acute phase.

LIST OF ABBREVIATIONS

°C	Degrees Celsius
ACE2	Angiotensin-converting enzyme 2
AdV	Adenoviral vector
ATIII	Antithrombin III
aTTP	Acquired thrombotic thrombocytopenic purpura
BH correction	Benjamini-Hochberg correction
BLI	Biolayer interferometry
Bmax	Maximal binding capacity
bPF4	Biotinylated-PF4
BSA	Bovine serum albumin
COVID-19	Coronavirus disease 2019
CVST	Cerebral venous sinus thrombosis
DNA	Deoxyribonucleic acid
DVT	Deep vein thrombosis
EDC	1-Ethyl-3-[3-dimethylaminopropyl] carbodiimide hydrochloride
EGF	Epidermal growth factor
FGF	Fibroblast growth factor
FI	Fluorescence intensity
Flt-3	Fms-like tyrosine kinase 3
GP	Glycoproteins
GRO α	Growth regulated oncogene α
HIT	Heparin-induced thrombocytopenia
IgG	Immunoglobulin G
IgG1	Immunoglobulin G1 subclass
IL	Interleukin
IL-1RA	IL-1 receptor antagonist
IP-10	Interferon gamma-induced protein 10
ITP	Immune thrombocytopenic purpura
K _D	Equilibrium dissociation constant
kDa	Kilodaltons
k _{off}	Dissociation rate constant
k _{on}	Association rate constant
mAb	Monoclonal antibody
MCP	Monocyte chemotactic protein
MDC	Macrophage-Derived chemokine
MGUS	Monoclonal gammopathy of undetermined significance
MIG	Monokine induced by interferon-gamma
MIP	Macrophage inflammatory protein
MM	Multiple myeloma
mRNA	Messenger ribonucleic acid
NaCl	Sodium chloride
NaOH	Sodium hydroxide
NET	Neutrophil extracellular trap
PBMC	Peripheral blood mononuclear cells

PBS	Phosphate buffered saline
PDGF	Platelet-derived growth factor
PE	Pulmonary embolism
PF4	Platelet factor 4
RANTES	Regulated-on-activation normal T-cell expressed and secreted
RU	Response unit
s-NHS	N-hydroxysulfosuccinimide
SARS-CoV-2	Severe acute respiratory syndrome coronavirus-2
sCD40L	Soluble CD40 ligand
SD	Standard deviations
spHIT	Spontaneous heparin-induced thrombocytopenia
SPR	Surface plasmon resonance
SVT	Splanchnic vein thrombosis
TD	T cell-dependent
TGF	Transforming growth factor
TI	T cell-independent
TNF	Tumor necrosis factor
VEGF	Vascular endothelial growth factor
VITT	Vaccine-induced immune thrombotic thrombocytopenia
VTE	Venous thromboembolism
vWF	von Willebrand factor

DECLARATION OF ACADEMIC ACHIEVEMENT

All the experiments detailed in this thesis were conducted by Yi Zhang under the supervision of Dr. Ishac Nazy, Dr. Donald M. Arnold, Dr. Sara Andres, and Dr. Zhou Xing with the following exceptions: surface plasmon resonance experiments were performed with the assistance of Dr. James Fredenburgh, and T-test comparisons of cytokine levels were performed by Dr. Anna Dvorkin.

1.0 INTRODUCTION

1.1 COVID-19 pandemic and vaccination efforts

The coronavirus disease 2019 (COVID-19) pandemic, caused by the severe acute respiratory syndrome coronavirus 2 (SARS-CoV-2), has led to significant global health challenges. Since its emergence in December 2019,¹ the virus has led to caused widespread illness and death, straining healthcare systems and impacting economies worldwide.² The rapid spread of the virus highlighted the need for effective vaccines to reduce severe symptoms and fatalities, and to achieve herd immunity by inducing neutralizing antibodies against the virus, thereby controlling the pandemic.^{3,4} This urgency accelerated vaccine development using various platforms.⁵ Whereas vaccines traditionally require a timeline of 10 to 15 years to develop,⁶ various SARS-CoV-2 vaccines have been created at unprecedented speed using novel platforms.

1.2 Adverse events associated with SARS-CoV-2 vaccination.

As vaccination efforts continue, there has been an increase in reported adverse events.⁷ The most common include mild localized reactions at the injection site, such as pain, redness, and swelling, as well as systemic effects like fatigue, headache, and muscle or joint pain.⁷ Although rare, serious adverse events have also been reported for both mRNA and adenovirus-vector-based vaccines. Vaccination with mRNA SARS-CoV-2 vaccines has been found to lead to an increased incidence of myocarditis (inflammation of the heart muscle) and pericarditis (inflammation of the outer lining of the heart).⁸ Additionally, a few cases of ulcerative colitis have been reported following these vaccinations.⁹

Symptoms of colitis include abdominal pain, diarrhea, and rectal bleeding, with flare-ups also occurring in patients with pre-existing inflammatory bowel disease.¹⁰ Vaccination with AdV-based vaccines, on the other hand, has been associated with an increased incidence of Guillain-Barré Syndrome, characterized by muscle weakness and paralysis.¹¹ Furthermore, these vaccines have also been linked to a rise in platelet-directed autoimmune phenomena, including immune thrombocytopenic purpura (ITP) and acquired thrombotic thrombocytopenic purpura (aTTP).^{12,13} ITP typically presents with severe isolated thrombocytopenia, often with platelet counts around $10 \times 10^9/L$, and is more likely to present with bleeding rather than thrombosis.^{12,14} aTTP is associated with autoantibodies that promote the clearance of the ADAMTS13 protein, resulting in excessive clumping of platelets and the formation of platelet thrombi within the microcirculation.¹³ Despite these rare conditions, there have been numerous reports of concurrent thrombosis and thrombocytopenia following AdV-based SARS-CoV-2 vaccination, raising significant safety concerns about these vaccines.¹²

1.3 Adverse effects following Adenoviral vector (AdV)-based vaccine administration.

In April 2021, Greinacher *et al.*,¹⁵ Scully *et al.*,¹⁶ and Schultz *et al.*¹⁷ reported the earliest cases of thrombosis and thrombocytopenia following a primary-dose vaccination with ChAdOx1-S in otherwise healthy individuals. The index patient reported by Greinacher *et al.* presented in late February with pulmonary embolism (PE) and portal vein thrombosis, accompanied by elevated D-dimer levels, low fibrinogen, and severe thrombocytopenia ($18 \times 10^9/L$, normal

range $150 - 400 \times 10^9/L$).¹⁵ Despite receiving treatments such as low molecular weight heparin and platelet transfusion, she passed away 11 days post-vaccination.¹⁵ Subsequently, Muir *et al.* reported a similar clinical syndrome following the first dose of Ad26.COVS vaccine.¹⁸ The patient, who was hospitalized 14 days post-vaccination, exhibited extensive disseminated intravascular coagulation associated with severe thrombocytopenia ($13 \times 10^9/L$).¹⁸ Clinical presentations included splanchnic vein thrombosis (SVT) and cerebral venous sinus thrombosis (CVST), which is also accompanied by elevated D-dimer levels and low fibrinogen.¹⁸ These cases underscore the emerging concerns around AdV-based vaccines and their potential link to inducing a prothrombotic state, warranting a deeper understanding of the pathogenic mechanisms involved.

This newly recognized prothrombotic adverse effect associated with AdV-based SARS-CoV-2 vaccines was later termed vaccine-induced immune thrombotic thrombocytopenia (VITT), most notably following administration of the ChAdOx1-S and Ad26.COVS vaccines.¹⁵ As of April 2022, over 2 billion doses of ChAdOx1-S have been administered, with an associated risk of VITT of 3.2 - 16.1 cases per million doses.¹⁹ In contrast, with over 50 million doses administered, Ad26.COVS is associated with a lower risk of VITT, estimated at 1.7 – 3.7 cases per million doses.²⁰ Notably, there were no reported cases of VITT associated with any other Ad26-vectored vaccines developed by Janssen, such as Ad26.ZIKV and Ad26.HIV, with the exception of the SARS-CoV-2 vaccine.^{21,22} However, it's important to consider that these other vaccines are still in clinical trials and have not been administered to populations on the same scale as the SARS-CoV-2

vaccines.^{21,22} This absence of VITT cases may suggest unique mechanisms associated with the SARS-CoV-2 vaccine or reflect an undetected occurrence due to the smaller sample sizes in the trials.

The prothrombotic nature of VITT is intricately linked to platelet activation and the subsequent thrombi formation. Platelets are anuclear immune cells integral to hemostasis.²³ Humans generate approximately 10^{11} platelets daily in the bone marrow through a process called thrombopoiesis,²³ with a typical lifespan of 7 – 10 days in circulation.²⁴ Upon vascular injury, the plasma-circulating, resting platelets encounter exposed collagen and von Willebrand factor (vWF) in the subendothelial matrix, triggering their activation and adhesion to the vascular walls.²⁴ This initial adhesion initiates intracellular signaling pathways, leading to a shape change from discoid to rounded with pseudopodia extensions, expanding their surface area for further interactions with other platelets and the subendothelial matrix.²⁴ Activated platelets release granular contents that further recruit and activate additional platelets,²⁴ leading to their aggregation and the formation of a platelet plug, which stabilizes the initial hemostatic response.²⁴

Platelet activation involves multiple biochemical processes, including the production of thromboxane A₂ to amplify platelet activation,²⁵ changes in membrane phospholipids to increase the expression of integrin α IIb β 3 (GPIIb/IIIa) receptors for fibrinogen interaction and additional platelet recruitment, and the release of granular contents such as PF4, fibrinogen, and vWF.²⁵ These processes amplify platelet activation and aggregation, stabilize the growing platelet plug, and propagate the coagulation cascade, leading to fibrin formation and stable clot development at the site of vascular injury.²⁵ In prothrombotic conditions, however,

cell-mediated mechanisms can lead to platelet activation and aggregation without the presence of overt vascular injury.²⁵

1.4 AdV-based vaccines

The spike protein was identified in 2020 as the primary target for SARS-CoV-2 vaccine development due to its capacity to elicit neutralizing Immunoglobulin (IgG) antibodies,²⁶ which inhibit the binding of spike protein to the angiotensin-converting enzyme-2 (ACE2) receptor and reduce viral infectivity of host cells.²⁶ Coronaviruses, including SARS-CoV-2, are a type of enveloped RNA virus distinguished by the expression of spike glycoproteins on their surface.²⁷ Through their receptor-binding domain, the spike proteins enable the virus to infect host cells by binding to the ACE2 receptor on the cell surface.²⁷ Once bound, the virus is endocytosed into the host cell, where the viral envelope fuses with the endosomal membrane, releasing the viral RNA into the cytoplasm for viral protein translation and assembly of new viral particles.²⁷ Given the crucial role of the spike protein in SARS-CoV-2 infectivity, it became the focal point for vaccine development.

AdV-based vaccines, such as the ChAdOx1-S (AstraZeneca) and Ad26.COV2.S (Johnson & Johnson/Janssen), use replication-deficient adenoviral vectors to deliver dsDNA encoding the SARS-CoV-2 spike protein into host cells via receptor-mediated endocytosis.^{28,29} Once inside the cell, the DNA is transported to the nucleus for transcription, and the resulting mRNA is later translated into the spike protein in the cytoplasm.³⁰ Some of the expressed spike proteins are digested into fragments, which are then presented on the host cell surface and by antigen-

presenting cells via major histocompatibility complexes.³¹ This process elicits the production of neutralizing antibodies by activated B cells.³⁰ As DNA is inherently more stable than mRNA, and the protective viral capsid shell further enhances stability, AdV-based vaccines can be stored at 2 – 8 degrees Celsius (°C) for three to six months,³⁰ making them more suitable for storage and use in regions with limited refrigeration infrastructure.

1.5 Heparin-induced thrombocytopenia (HIT)

The distinct clinical presentation of VITT, characterized by thrombocytopenia and thrombosis resembles another prothrombotic disorder known as spontaneous heparin-induced thrombocytopenia (spHIT), a rare variant of a well-studied disorder called HIT.³²

HIT is an immune-mediated prothrombotic syndrome paradoxically caused by the formation of an immunogenic complex between the endogenous protein platelet factor 4 (PF4) and the widely prescribed anticoagulant heparin.³³ It is characterized by thrombocytopenia and an increased risk of thrombosis, with a thrombosis-associated mortality rate of 20 – 30%.³³ Heparin is a negatively charged glycosaminoglycan utilized extensively in cardiac and orthopedic surgeries due to its reversibility, non-toxicity, and biodegradability.^{34,35}

During thrombosis and platelet activation, the effect of heparin can be diminished due to its interaction with the platelet-secreted protein of PF4.³⁶ PF4 is a chemokine released from α -granules within platelets during platelet activation.³⁷ The circulating level of PF4 is low (1.8 ng/ml) compared with the amount contained within platelets ($18 \pm 4 \mu\text{g}/10^9$ platelets), but can exceed 600 ng/mL following

platelet activation.³⁸ PF4 is a tetrameric protein with each monomer composed of 70 amino acids with a molecular weight of 7.8 kilodaltons (kDa).³⁷ PF4 maintains a dynamic equilibrium between monomeric, dimeric, and tetrameric forms.³⁹ The tetrameric structure predominately implicated in multiple immune-mediated disorders.³⁹ This tetrameric form of PF4 is composed of two asymmetric dimers, forming a cylindrical structure with an equatorial ring of positively charged amino acids.³⁸

PF4 binds to negatively charged cell surfaces due to its cationic nature, primarily to glycosaminoglycan moieties on heparan sulfate, thereby modulating cell-mediated inflammatory responses in endothelial cells, neutrophils, and monocytes.³⁶ Heparan sulfate functions as an anticoagulant by interacting with antithrombin III (ATIII), which significantly increases ATIII's ability to inhibit thrombin and factor Xa, preventing their participation in the clotting cascade and thereby fibrin clot formation.⁴⁰ On cell surface, PF4 competes with ATIII for binding to heparan sulfate, reducing the anticoagulant efficiency of ATIII and thereby contributing to the overall prothrombotic nature of PF4.⁴⁰ Additionally, the cationic property of PF4 enables its interaction with bacterial lipopolysaccharides and teichoic acids, which is proposed to exert protective properties by facilitating bacterial neutralization and immune clearance, suggesting a potential role for PF4 in antibacterial host defense.⁴¹

Given the structural and charge similarity to heparan sulfate, heparin's anticoagulant effect is primarily mediated by enhancing ATIII activity.⁴⁰ Additionally, heparin and PF4 interact with ultra-high affinity with an equilibrium dissociation constant (K_D) of 30 nM due to charge complementarity.³⁶ This

electrostatic interaction neutralizes the negative charge of heparin, reducing its ability to activate ATIII and thereby diminishing its anticoagulant efficacy. Moreover, heparin binding stabilizes PF4 in its tetrameric state, causing the exposure of neoepitopes on PF4³⁹ and subsequent antibody production in a subset of heparin recipients, predominantly of the immunoglobulin G1 subclass (IgG1).^{42,43} This electrostatic interaction neutralizes heparin's negative charges, reducing its ability to activate ATIII and thereby diminishing its anticoagulant efficacy.³⁶ This unique combination of heparin and PF4 are central to the immunogenic complex formation in HIT.

The frequency of anti-PF4/heparin IgG antibody development varies based on clinical settings. These antibodies can develop in approximately 0.6% of general medical patients,⁴⁴ while surgical patients, particularly those undergoing orthopedic or cardiac surgery, face a significantly higher risk.⁴⁵ Notably, this frequency approaches 50% in patients undergoing cardiopulmonary bypass surgery.⁴⁶ However, HIT involves a polyspecific immune response, where polyclonal anti-PF4/heparin antibodies bind to multiple sites on the PF4 molecule.⁴⁷ Many of these sites are non-pathogenic and their engagement does not cause platelet activation or further aggregation.⁴⁸ Consequently, while anti-PF4 antibodies can form in a larger patient population, only 0.2 – 3% of these patients develop platelet-activating antibodies that facilitate clot formation.⁴⁹

Using a PF4-mutant library with each amino acid individually mutated through alanine mutagenesis, Huynh *et al.* identified multiple binding sites for HIT antibodies on PF4 in different HIT patient sera via epitope mapping.⁵⁰ This approach allowed for the pinpointing of five key amino acids in a localized region

on PF4 critical for the binding of pathogenic HIT antibodies.⁵⁰ These antibodies are responsible for platelet activation and the clinical symptoms of HIT, distinguishing them from non-pathogenic antibodies that recognize different areas across PF4, which can be present following heparin administration but do not cause symptoms and disease.⁵⁰

The structural basis of antigenic complexes in HIT and their interaction with anti-PF4 antibodies was revealed through X-ray crystallography. The site for anti-PF4/heparin antibodies engagement is exposed when PF4 complexes with long polyanions.³⁹ These polyanions, such as heparin, force PF4 tetramers into proximity, stabilizing the structure necessary for antibody binding.³⁹ Specifically, heparin binds to the “closed” end of the PF4 tetramer, revealing and stabilizing the epitope for pathogenic antibodies on the “open” end.³⁹ This work was performed by using the HIT-mimicking monoclonal antibody known as KKO, which binds to this stabilized epitope on the PF4 tetramer, enhancing the formation of large antigenic complexes that are characteristic of HIT, leading to platelet activation.³⁹

Upon production, the HIT antibodies form immune complexes with PF4/heparin that interact with immune cells, including platelets, neutrophils, and monocytes, via surface FcγRIIA receptors.⁵¹ The FcγRIIA receptor is a transmembrane, low-affinity receptor that recognizes the Fc portion of IgG antibodies when they are complexed with antigens.⁵¹ Platelet activation by HIT antibodies through FcγRIIA was confirmed by blocking the receptor with IV.3, a monoclonal antibody against FcγRIIA.⁵¹ This blockade halted HIT antibody-mediated platelet activation, proving the specificity of the interaction.⁵¹ The large immune complexes formed in HIT, where one heparin molecule bridges two PF4

tetramers,³⁹ facilitate the crosslinking of multiple FcγRIIA receptors on platelets.³⁹ This receptor clustering triggers signal transduction via an intracellular immunoreceptor tyrosine-based activation motif, leading to platelet activation and aggregation, contributing to the prothrombotic characteristic of HIT.⁵¹

1.6 Vaccine-induced immune thrombosis and thrombocytopenia (VITT)

1.6.1 Clinical and laboratory features of VITT

VITT is a rare but severe adverse condition associated with adenovirus-based SARS-CoV-2 vaccines marked by thrombosis and mild to severe thrombocytopenia (median platelet count of $50 - 80 \times 10^9/L$).⁵² While HIT typically presents with thrombosis in common locations like deep vein thrombosis (DVT) and pulmonary embolism (PE),⁵³ VITT is characterized by thrombi formation in both venous and arterial systems, often at atypical sites such as cerebral venous sinus thrombosis (CVST) and splanchnic vein thrombosis (SVT).^{15,16} Despite being a rare cerebrovascular condition affecting approximately 3 per 100,000 individuals in the general population,⁵⁴⁻⁵⁶ a case series has described CVST in 50 – 82% of VITT patients and is associated with a 2.7-fold higher risk of mortality due to accompanying intracranial hemorrhaging.^{15-17,57}

The similarities in clinical presentation, including thrombosis and thrombocytopenia, between VITT and sPHIT prompted testing that led to the discovery of platelet-activating anti-PF4 antibodies in VITT patients. Nearly all reported VITT cases have tested positive for anti-PF4 antibodies in immunoassays, showing results with high optical densities greater than 2.0 to 3.0.¹² This suggests a resemblance between these pathogenic antibodies and potentially similar

mechanisms underlying their development.⁵⁸ These pathogenic antibodies induce a hypercoagulable state, leading to symptoms such as severe headache, blurred vision, persistent chest or abdominal pain, shortness of breath, and unusual bruising or bleeding.^{12,59} However, unlike the HIT antibodies whose antigen is the PF4/heparin complex, VITT antibodies were shown to induce significant platelet activation in the absence of heparin, indicating its specificity towards PF4 alone.^{15,17,60}

1.6.2 Characteristics of VITT anti-platelet factor 4 (PF4) antibodies

Contributing to their clinical similarities, both VITT and HIT involve predominantly IgG1 antibodies that induce platelet activation through the FcγRIIa receptor.⁶¹ Moreover, both disorders involve rapid development of anti-PF4 antibodies. Symptoms can appear as early as five days post-heparin exposure in HIT⁴⁵ and four days post-vaccination in VITT.¹² The rapid development challenges the typical timeframe for T-cell-dependent B cell stimulation and antibody production, which generally peaks between 7 and 14 days.⁶² Instead, given anti-PF4 antibodies are predominantly IgG, it raises the question of whether this is a T-independent B cell response, which can generate a short burst of low-affinity antibodies peaking between three to five days post-antigen encounter;⁶² or if these patients have preexisting immune memory targeting PF4, with vaccination merely triggering the activation of these B cell clones.⁶³ Understanding the nature of these antibodies could provide valuable insights into their development and underlying mechanisms.

However, several key differences in the characteristics of VITT and HIT antibodies highlight distinct pathophysiological mechanisms. While HIT antibodies

are polyclonal,⁴⁷ with only a subset binding to the pathogenic region on PF4 and lead to platelet activation,⁴⁹ resulting in variable pathogenic potential among patients,⁴⁹ VITT antibodies are more consistently pathogenic.⁶⁰ Once anti-PF4 antibodies are detected in VITT patients, they are predominantly platelet-activating and highly likely to induce clot formation, indicating a more uniform pathogenic profile.⁶⁰

Another notable difference is the requirement for inducing platelet activation. HIT antibodies necessitate the presence of a PF4/heparin complex not only for antibody formation but also for activating platelets.⁶⁴ In contrast, VITT antibodies can activate platelets with PF4 alone, without the need for polyanionic substances like heparin or the AdV-based vaccines.⁶⁵ Whether the formation of an immunogenic complex with the vaccine particle, as is the case in HIT, leads to VITT antibody production remains poorly understood. Therefore, while AdV-based vaccination is implicated in the production of these antibodies, the precise mechanisms and contributing factors remain to be investigated.

1.6.3 Proposed pathogenic mechanisms of VITT and conflicting findings.

Although endogenous PF4 alone can lead to platelet activation once VITT anti-PF4 antibodies are formed, the pathogenic mechanism underlying the development of these antibodies remains widely debated. The role of SARS-CoV-2 AdV-based vaccines in the formation of these antibodies, or whether vaccine exposure alone is sufficient for their generation, is not fully understood. Therefore, the origin of anti-PF4 antibodies in VITT and the relationship with AdV-based vaccines and PF4 require further investigation.

One hypothesis suggests that VITT anti-PF4 antibodies may develop through a sequence of events comparable to HIT antibodies, through neoepitope formation following PF4 interaction with polyanionic substances in the vaccine preparation.^{66,67} This could involve the interaction between PF4 and the polyanionic AdV-based vaccine vector via their negatively charged hexon capsid proteins in the bloodstream following vaccine administration.^{66,67} It is proposed that a small amount of AdV particles may enter the bloodstream through minor capillary damage following vaccine administration.⁶⁷⁻⁶⁹ These polyanionic AdV capsid proteins can bind to the cationic PF4, similar to their interaction with heparin in HIT, thereby exposing neoantigens on PF4 capable of stimulating an immune response. These PF4/AdV complexes may be transported to the lymphatic system by monocytes and macrophages, serving as the immunogen by stimulating the differentiation of pre-existing anti-PF4 B cells, leading to the formation of pathogenic anti-PF4 IgG antibodies.⁶⁷⁻⁶⁹

In support of this hypothesis, multiple studies have demonstrated interactions and potential complex formation between PF4 and AdV-based vaccines. Baker *et al.* identified electrostatic interactions between PF4 and both AdV-based SARS-CoV-2 vaccines, noting that PF4 interacts more frequently with ChAdOx1 compared to the Ad26 capsid due to its higher electronegativity.⁶⁸ Moreover, Greinacher *et al.* demonstrated the co-localization of PF4 and ChAdOx1-S hexon particles in close proximity to anti-PF4 antibodies using various microscopy techniques, reinforcing the complex involvement underlying VITT antibody formation.⁶⁷

However, contradictory opinions have emerged, questioning whether PF4 actually binds to the AdV capsid, or alternative mechanisms are involved for VITT antibody formation. Although both AdV-based vaccines have been associated with VITT incidences, a study using dynamic light scattering observed aggregation between PF4 and the ChAdOx1-S vaccine preparations but not with Ad26.COV2.S.⁶⁹ Moreover, no aggregates formed when PF4 was combined with purified virions of ChAdOx1-S or Ad26.COV2.S.⁶⁹ These results suggest that PF4 may be binding to the free protein components of the vaccine and other cofactors may contribute to inducing the anti-PF4 immune response.⁶⁹ Therefore, these contradicting observations raise questions about the PF4/AdV complex formation found previously by Baker *et al.*, compelling us to investigate this interaction more thoroughly across both AdV-based SARS-CoV-2 vaccine platforms. Understanding these mechanisms is crucial for guiding the design of safer AdV-based therapeutic strategies and developing targeted interventions to mitigate the risk of such thrombotic complications.

Beyond neoepitope formation, contributing factors that could lead to excessive inflammation and potentially facilitate pathogenic anti-PF4 antibody production have also been proposed. These factors are primarily attributed to the excipients and production-related impurities of the vaccines. Proteomic analysis via mass spectrometry has revealed substantial amount of human cell line proteins in ChAdOx1-S, with levels varying from 44 – 70% across different lots,⁶⁹ in contrast to 0.26 – 0.96% found in Ad26.COV2.S.⁷⁰ These impurities include heat-shock proteins, which are recognized by the immune system as signals of cellular stress or damage and may contribute to platelet activation at the site of vaccine injection.⁶⁹

Two stabilizers used in these vaccines may also contribute to the inflammatory response. Ethylenediaminetetraacetic acid in ChAdOx1-S can increase vascular permeability, potentially leading to lead to dermal vessel leakage and therefore facilitating the spread of proinflammatory factors, such as cytokines.^{67,69} However, considering that VITT typically manifests between 5 to 30 days post-vaccination—a period during which the vaccine excipients are likely no longer in circulation,⁵⁷ these components are unlikely to contribute to VITT pathogenesis.⁷¹ Therefore, we are considering whether other contributors, such as a hyperinflammatory state and proinflammatory cytokines, may play a role in VITT severity and antibody generation in addition to the neoepitope formation.

1.7 Cytokine involvement in thrombotic disorders

It is clear that the development of VITT antibodies and the associated thrombotic pathogenesis depends on the activation of the adaptive immune system through intricate signaling interactions with the innate immune system. Cytokines, as pivotal mediators of immune responses,⁷² could play a crucial role in modulating the inflammatory environment that facilitates the development of anti-PF4 antibodies and induces the severe clotting characteristic seen in VITT patients. Understanding the cytokine profiles of VITT patients may provide deeper insights into the pathogenesis of VITT.

Cytokines are elaborate cell-secreted factors that bridge the innate and adaptive immune systems.⁷² They can be secreted by both immune and non-immune cells and act on the secreting cell itself, on nearby cells, or on distant cells through the bloodstream, via cytokine-specific receptors on the cell surface.⁷² These

inducible molecules can mediate various cellular processes depending on the situation, such as the expansion and maturation of lymphocytes, development of antibodies, and activation of endothelial cells and innate immune cells like macrophages and neutrophils.⁷²

1.7.1 Implication of proinflammatory cytokines in venous thrombosis

Inflammation and coagulation are closely interconnected processes crucial for hemostatic regulation, with the balance between host defense and tissue function restoration being regulated by proinflammatory and anti-inflammatory/regulatory cytokines.⁷² However, production of excessive proinflammatory cytokines or insufficient regulatory cytokines can create a heightened inflammatory response, leading to tissue damage and exacerbating disease severity.⁷³

The role of proinflammatory cytokines in venous thromboembolism (VTE) has been extensively explored in previous studies.^{74,75} These cytokines mediate various acute phase responses, thereby promoting the development of a stable clot. For example, interleukin (IL)-1 β and IL-6 induce the activation of endothelial cells to upregulate adhesion molecules, promoting the migration of immune cells to the site of thrombosis.^{74,75} IL-1 α and soluble CD40 ligand (sCD40L)⁷⁶ induce the activation of platelets to promote degranulation and secretion of PF4, thereby promoting thrombus formation by decreasing the anticoagulant efficiency of heparan sulfate.⁷⁴ Elevated levels of IL-6 and IL-8,^{74,75} in particular, have been consistently found in patients with VTE, such as deep vein thrombosis (DVT),^{74,75} actively participating in the pathogenesis of the disease. This established role of

cytokines in VTE prompts further exploration of their involvement in VITT severity and pathogenesis.

However, despite extensive studies on cytokines associated with various types of VTE, the role of the proinflammatory environment contributing to VITT severity and pathogenesis has not been thoroughly investigated. In the existing literature, cytokine profiling has only been performed on one VITT patient who experienced stroke following ChAdOx1-S vaccination.⁷⁷ She was found to have significantly elevated levels of proinflammatory cytokines IL-1 β , MCP-1, IL-5, and IP-10 in comparison to stroke patients without VITT.⁷⁷ However, VITT pathogenesis may also mirror that of HIT, being induced by a loss of immune regulation rather than hyper-inflammation.⁷⁸ In a cytokine profile study involving 10 HIT patients, lower levels of regulatory cytokine IL-10 and transforming growth factor (TGF)- β 1 were observed in compared to healthy controls without heparin-exposure, suggesting the contribution of immune dysregulation towards HIT pathogenesis.⁷⁸

Beyond tissue injuries, heparin exposure and AdV-based vaccination have also been shown to affect cytokine profiles, therefore should be controlled for in cytokine analysis. Heparin functions as an anti-inflammatory agent by binding to cytokines such as IL-6,^{79,80} IL-12,⁸¹ and IFN- γ ,⁸⁰ thereby reducing their availability for activation of signaling pathways. It also directly inhibits the production of these cytokines by suppressing the expression of the inflammatory transcription factor NF- κ B, thereby mitigating inflammation.⁸⁰ In contrast, vaccination of rhesus monkeys with chimpanzee adenovirus serotype 155 vaccines consistently promotes an IFN-associated signature,⁸² characterized by elevated levels of interferon

gamma-induced protein 10 (IP-10) and monokine induced by gamma interferon (MIG) seven days post-vaccination.⁸² Similarly, vaccination with the Ad26 vector induces a robust IFN response, increasing cytokines such as IFN- γ and IP-10,⁸³ along with inflammatory-related cytokines IL-1RA and IL-6.⁸³

Although it is no longer possible to determine whether these cytokine elevations precede VITT or are a consequence of it, identifying the cytokine environment of VITT patients can enhance our understanding of VITT pathogenesis, gaining insights into the potential mechanisms driving the severity of this disorder.

1.7.2 Cytokine involvement in B-cell activation and antibodies development

Beyond a shared inflammatory environment, which may be present in both HIT and VITT patients during anti-PF4 development, the oligoclonal feature of VITT antibodies⁶¹ and the distinctive clotting profile of VITT patients¹⁵ raised the question: what supports such a unique development? As cytokines act as essential cofactors in antibody production and the differentiation of naïve B cells into plasma cells,⁸⁴ the cytokine profiles of VITT patients may provide insight into this process. Since the mechanisms underlying the rapid development of IgG anti-PF4 antibodies in VITT remain unknown, we investigated cytokines that might be involved in T-dependent and T-independent B cell response pathways. By analyzing the cytokine profiles, we aim to depict the specific immune responses that contribute to the pathogenesis and severity of VITT.

During T-dependent B cell activation, cytokines IL-4, IL-6, and IL-21 play crucial roles in the stimulation, survival, and differentiation of B cells. IL-4

provides costimulatory signals that initiate T-dependent (TD) response by inducing the growth of B cells engaged by T helper cells.⁸⁵ IL-21 promotes the survival of high-affinity B cells by increasing the expression of anti-apoptotic proteins during the somatic hypermutation and affinity maturation of activated B cells.⁸⁶ Additionally, IL-21 directly promotes the differentiation of activated B cells into plasma cells.⁸⁴ IL-6 further supports this process indirectly by inducing the expression of IL-21,⁸⁷ creating a supportive environment that enhances B cell differentiation and antibody production.

On the other hand, T-independent (TI) B cell activation can be further divided into TI-1 and TI-2 responses. TI-1 antigens, such as bacterial LPS, can induce polyclonal B cell activation through engagement of pattern recognition receptors. TI-2 antigens, in contrast, are typically highly repetitive structures that can interact with and cross-link numerous B-cell surface receptors, driving an oligoclonal B cell response similar to those seen in VITT.⁸⁸ This TI-2 type activation is further enhanced by cytokines such as IL-2,⁸⁹ IL-5,⁸⁹ and IL-21,⁹⁰ which are produced by dendritic cells or natural killer cells.^{89,90} However, instead of IgG development, TI-2 response is most commonly associated with strong IgM production in the context of bacterial infections, often triggered by bacterial surface polysaccharides and polymerized flagellin.⁸⁸

2.0. RESEARCH OUTLINE

2.1. Aim

This work aims to identify key elements associated with the pathogenesis of VITT: 1) the possible complex formation between PF4 and AdV-based SARS-

CoV-2 vaccines, which could lead to the development of the VITT immunogen; and 2) the correlation of cytokines with anti-PF4 antibody development and disease severity.

2.2. Rationale

The mechanisms underlying VITT pathogenesis remain widely debated. Theories suggest that these antibodies may form through a sequence of events similar to HIT, where PF4 interacts with polyanionic hexons of the adenoviral vector, much like its interaction with heparin in HIT.^{66,67} This interaction forms neoepitopes on the surface of PF4, which act as immunogens to induce anti-PF4 antibody formation.^{66,67} However, conflicting evidence exists regarding the role of AdV-based vaccines in the formation of VITT antibodies from PF4 interactions.^{68,69,91} Some studies suggest that ChAdOx1-S can bind to PF4,⁶⁸ while Ad26.COVS2.S does not,^{69,91} despite both vaccines have led to the development of VITT and pathogenic anti-PF4 antibodies.^{19,20} This raises the question of whether the PF4 interaction is truly responsible for antibody formation, or if another mechanism triggered by vaccine administration is at play. Additionally, the cytokine profile of VITT patients has not been extensively studied, even though cytokines are known to play roles in both antibody formation and venous thrombosis,^{74,75,84} which are key characteristics of VITT. Therefore, the potential correlation of cytokine activity to VITT antibody development and disease severity warrants further investigation. Comparison to HIT pathology which could yield further insights in the developments of both pathologies. Such insights are essential for the continued use of the AdV platform in future vaccine development, given

their stability and suitability for storage at higher temperatures,³⁰ which is beneficial for countries lacking ultra-low temperature storage facilities.

2.3. Hypothesis

VITT takes place concurrently with the following events:

1. PF4 interacts with both ChAdOx1-S and Ad26.COv2.S AdV-based SARS-CoV-2 vaccines.
2. VITT occurs during a state of elevated proinflammatory cytokine production, which correlates with the formation of anti-PF4 antibodies and disease severity.

2.4. Objectives

(i) Evaluate the interactions between PF4 and AdV-based SARS-CoV2 vaccines

To assess the interaction between PF4 and both ChAdOx1 and Ad26.COv2.S vaccines, we employed two optical techniques: Surface Plasmon Resonance (SPR) and Biolayer Interferometry (BLI). Both BLI and SPR are optical detection techniques designed to assess the interaction dynamics between two molecules: a ligand and an analyte.⁹² The ligand is immobilized on the detection sensor—on a sensor chip for SPR, and on the sensor tip for BLI—while the analyte is present in the assay buffer.⁹² BLI employs optical fibers to measure differences in reflected light frequencies between a reference biolayer and a layer for molecule attachment, with the thickness of the biofilm altered by molecule attachment or binding.⁹² The interference pattern generated by the two reflected light frequencies with the incident light is displayed as the relative displacement intensity (nm).⁹² In contrast, SPR operates as a flow-based method, directing the analyte in the buffer

phase over the immobilized ligand on the sensor.⁹² In this technology, a conductive gold film on the sensor becomes excited by incidence light at a specific angle.⁹³ When the analyte binds to the ligand attached to the sensor surface, the local refractive index at the interface between the gold film and the assay buffer changes proportionally to the change in mass at the sensor surface.⁹³ This shift in refractive index is detected as a change in the resonance angle, which is measured in response units (RU).⁹³ Although both BLI and SPR are effective for detailed kinetic studies, with BLI offering high throughput screening, SPR provides superior sensitivity and reproducibility, particularly for low molecular weight analytes.⁹⁴ BLI's limitations, such as upward drifts in dissociation curves due to sample evaporation,⁹⁵ affect the accuracy of high-affinity interaction analysis and further highlight the performance gap. Additionally, experimental variability between the two technologies has limited the correlation between interaction parameters obtained by the two technologies.⁹⁶ To confirm the interaction, both PF4 and AdV-based vaccines were alternatively used as the analyte and the ligand in interaction analyses using both optical techniques, aiming to observe a reversible interaction when the roles of ligand and analyte are switched. As an additional control, we introduced another Janssen AdV-based vaccine against the ZIKA virus (Ad26.ZIKV), which shares the same vector as their SARS-CoV-2 vaccine.²¹ Despite being in clinical trials and having limited distribution compared to SARS-CoV-2 vaccines, there have been no reports of VITT following its administration.^{21,97}

(ii) Investigate cytokines involvement in VITT by determining whether they:

- Associate with the development of VITT antibodies.

- Demonstrate specificity to VITT antibody development or are implicated in other anti-PF4 antibody-mediated disorders.
- Correlate with the disease severity of VITT.

To investigate whether a proinflammatory environment contributes to anti-PF4 formation and disease severity in VITT, a comprehensive 48-plex cytokine analysis was performed on patient serum to detect circulating cytokine levels. This analysis included cytokines involved in various functions such as inflammation, immune regulation, colony stimulation, and antibody production, aiming to survey the overall cytokine environment in VITT patients, providing insights into processes that may underlie antibody production and disease progression. To explore the posted questions, we conducted three main comparisons of cytokine levels between: 1) VITT patients (VITTpos) who had CVST (VITTpos_CVST) and those who had thrombosis at other sites of the body (VITTpos_other); 2) VITTpos patients and those who experienced similar clinical symptoms following vaccine administration but did not test positive for anti-PF4 antibodies (VITTneg); and 3) VITTpos patients and HIT patients (HITpos), which are both anti-PF4 antibody-mediated disorders.

3.0 MATERIALS AND METHODS

3.1 Interaction analysis

3.1.1 BLI interaction assays

Experiments were performed using an Octet-QK Red 96 (FortéBio, USA) that was maintained at 25°C. Samples were agitated at 1000 revolutions per minute to address potential diffusion limitations of the analyte. The sensors were pre-

soaked for 10 min in 200 μL /well of the assay buffer, while the experiments were run with 200 μL /well of analyte buffer. Two negative controls were included in each experiment to eliminate nonspecific binding: assay buffer in place of ligand and analyte, respectively; and assay buffer in place of the ligand only.

Streptavidin sensors (SA, Sartorius, Göttingen, Germany) were used when the PF4 acts as the ligand. The sensors were hydrated before establishing the initial baseline for 60 seconds. Increasing concentrations of biotinylated PF4 (bPF4) was loaded onto the sensors for 800 seconds before establishing the second baseline in the assay buffer for 600 seconds. The loaded sensors were then exposed to SARS-CoV-2 AdV-based vaccines for 1200 seconds at their stock concentrations (ChAdOx1-S: $1.2\text{E}12$ VP/mL; Ad26.COV2.S: $1\text{E}11$ VP/mL) to observe maximum interaction levels, if such interactions exist. The sensors were then submerged in assay running buffer for 1800 seconds while the dissociation rates were measured.

Amine coupling sensors (AR2G, Sartorius, Göttingen, Germany) were used when PF4 serves as the analyte. After establishing the initial baseline for 60s in UltraPure Distilled Water (UPW, Invitrogen, MA, USA), the carboxy-terminated surface was activated with 40mM of 1-Ethyl-3-[3-dimethylaminopropyl] carbodiimide hydrochloride (EDC, Sartorius, Göttingen, Germany) and 20mM of N-hydroxysulfosuccinimide (s-NHS, Sartorius, Göttingen, Germany) in UPW for 300 sec to generate reactive NHS esters. $1.2\text{E}12$ VP/mL of vaccines diluted in sodium acetate (pH 4.0; Sartorius, Göttingen, Germany) were loaded onto the sensors for 1200 seconds. The unreacted ester ends were then quenched in 1M ethanolamine (pH 8.5; Sartorius, Göttingen, Germany) for 300 seconds before establishing the second baseline for 120 seconds. Association with 7.5 $\mu\text{g}/\text{mL}$ of

PF4 was measured for 900 seconds, before which the dissociation was measured for 1800 seconds. These experimental steps are represented in the resulting sensorgrams as ligand association with the analyte (association), and analyte dissociation (dissociation) from the ligand. The ligand loading step is indicated in the sensorgram when no association between the ligand and the analyte is detected.

To demonstrate the sensitivity differences between BLI and SPR, 20 µg/mL of anti-hexon (Thermo Fisher Scientific, USA) diluted in sodium acetate (pH 6.0; Sartorius, Göttingen, Germany) was loaded onto the sensors for 720 seconds. After quenching and reestablishing the baseline in vaccine formulation buffer, as previously described, 1.2E12 VP/mL of ChAdOx1-S was loaded onto the sensors for 1200 seconds, followed by a baseline reestablishment for 300 seconds. Enrichment with 20 µg/mL of anti-hexon was then measured for 1200 seconds, and the dissociation was measured for 1800 seconds.

3.1.2 SPR interaction assays

Experiments were performed with the BIAcore T200 system. C1 sensor chips were used in a sandwiched setup when PF4 acts as the analyte. 400 – 600 RU of anti-hexon (ChAdOx1-S: Thermo Fisher Scientific, USA; Ad26.COVS.2.S and Ad26.ZIKV: Janssen, Netherlands) and monoclonal anti-PF4 (KKO) were immobilized onto the sensor chip using amine coupling. Immobilizations were carried out using HBS-EP and antibodies were diluted in acetate 4.5 buffer. Anti-hexon (Thermo Fisher Scientific, USA) was immobilized without being charged with vaccines to create a reference flow cell. For interaction analysis, vaccines were first injected for anti-hexon capturing. 100 – 130 RU of vaccine particles were

typically captured. For control experiments, a blank flow cell served as the background reference, whereas for vaccine interactions, the background reference was PF4 binding to anti-hexon, which was used to capture the vaccines onto the chip. Hence, their interaction responses may not be directly correlated.

CM4 sensor chips were used when the PF4 acts as the ligand. 7000 RU of streptavidin was immobilized onto the sensor chip using amine coupling in acetate 4.5 buffer. A reference flow cell was prepared by charging 20 RU of biotin, while the experimental cell was created by charging 400 – 500 RU of bPF4. Using the multicycle kinetics analysis protocol, serial dilutions of PF4, vaccines, or positive controls were prepared in HBS-EP buffer and flown over the captured ligands at 75 $\mu\text{L}/\text{min}$ with an association time of 60 seconds and a dissociation time of 600 seconds. A reference cell was created by adding biotin alone to mimic the background binding situation with the analyte in the experimental cell.

The flow cells were regenerated with 3M sodium chloride (NaCl) for 50 seconds at a flow rate of 50 $\mu\text{L}/\text{min}$, followed by a stabilization period of 120 seconds at the end of each cycle. NaCl was used for regeneration to avoid rupturing the particles, which triggers potential DNA-PF4 binding.

These experimental steps are represented in the resulting sensorgrams as analyte association (association) and dissociation (dissociation) from the ligand.

3.1.3 Data acquisition and statistical analysis

BLI data were acquired by the ForteBio Data Acquisition 9.0 Software version 9.0 and analyzed using the 1:1 homogenous analyte binding model with the ForteBio Data Analysis 9.0. Reference values from the control wells were

subtracted from the sample wells and all results were aligned to the baseline. The binding profile between each ligand and analyte was described in terms of wavelength shift (nm). The kinetic constants were calculated automatically by the data analysis software.

SPR data were collected by the BIAcore T200 Control Software, version 2.0, and binding affinities and maximum binding responses were determined by the BIAcore T200 Evaluation Software, version 1.0 via steady state approximation 10 seconds before injection stops. Values from the reference flow cell were subtracted from all experimental flow cells and all results were aligned to the response unit at baseline ($t = 0$). The binding profile between each ligand and analyte was described in terms of RU.

Binding affinities for the interactions were established through curve fitting of binding responses at each analyte concentration after equilibrium is stabilized. This nonlinear regression analysis leverages equilibrium binding data rather than kinetic model fitting, as the viral vectors have been shown to possess numerous binding sites across the viral capsid, predominantly within the interhexon spaces, complicating kinetic modeling.⁶⁸ Therefore, binding affinities are investigated instead of analyzing specific kinetic rates, such as association rate constant (k_{on}) and dissociation rate constant (k_{off}) parameters, to model the dynamic behavior of this interaction.

3.2 Cytokine profiling

3.2.1 Study design

To identify cytokines whose levels are unique to VITT, we compared them against several control groups: post-vaccination individuals whose vaccines received are nonspecific, and individuals with thrombotic thrombocytopenia syndrome (TTS) post-vaccination or heparin administration but not diagnosed with VITT or HIT serologically,

Serum samples were sent to the McMaster Immunology laboratory for diagnostic testing based on a clinical suspicion of either HIT or VITT during the initial symptom onset, forming the sample pool for this study. The suspected VITT cohort was subdivided into two groups according to laboratory serological results: those with platelet-activating anti-PF4 antibodies (VITTpos, n = 19) and those without (VITTneg, n = 11). Additionally, the VITTpos patients were categorized based on the presence of CVST into VITTpos_CVST (n = 10) for those experiencing CVST, and VITTpos_other (n = 9) for those experiencing thrombosis at other sites. A group of suspected HIT patients who were later diagnosed with platelet-activating anti-PF4/heparin antibodies (HITpos, n = 19) was also collected. However, the clinical diagnosis of these patients is unknown due to limited access to patient information.

3.2.2 Patient population

Patient characteristics are summarized in Table 1. Serum samples from suspected VITT patients were collected between 5 – 61 days post-vaccination with either the ChAdOx1-S or Ad26.COV2.S vaccines. The timing of serum collection

relative to heparin administration for the suspected HIT patients is unknown. The patient cohorts consist of a mix of genders and ages, with no statistically significant differences in these characteristics between the cohorts. However, platelet count data were unavailable for four patients in the VITtpos cohort.

3.2.3 Cytokine level testing

Serum samples from both the suspected VITT and HIT cohorts were analyzed for cytokine levels using a 48-panel Luminex assay conducted by Eve Technologies (Canada).

Cytokines being accessed include: Epidermal growth factor (EGF), fibroblast growth factor (FGF)-2, fms-like tyrosine kinase 3 ligand (Flt-3 ligand), platelet-derived growth factor (PDGF)-AA, PDGF-AB/BB, vascular endothelial growth factor (VEGF)-A, TGF- α , G-CSF, GM-CSF, M-CSF, Eotaxin, fractalkine, growth regulated oncogene α (GRO α), IL-8, monocyte chemotactic protein (MCP)-1, MCP-3, Macrophage-Derived chemokine (MDC), monokine induced by interferon-gamma (MIG), macrophage inflammatory protein (MIP)-1 α , MIP-1 β , regulated-on-activation normal T-cell expressed and secreted (RANTES), IL-2, IL-3, IL-5, IL-6, IL-7, IL-9, IL-12 (p40), IL-12 (p70), IL-15, IL-1 α , IL-1 β , interferon gamma-induced protein (IP)-10, IL-17A, IL-17E/IL-25, IL-17F, IL-18, IL-22, tumor necrosis factor (TNF)- α , TNF- β , IFN- α 2, IFN γ , soluble CD40 ligand (sCD40L), IL-4, IL-10, IL-13, IL-27, IL-1 receptor antagonist (IL-1RA).

3.2.4 Statistical analysis

Patient characteristics assessments were performed using Python (version 3.12.0). Patient sex distribution was then analyzed by the Fisher's Exact Test,

whereas age was assessed using independent two-sample t-test and presented as mean \pm standard deviations (SD). All cytokine level analyses were conducted using Log₂-transformed fluorescence intensity (FI) values obtained from Luminex assays.⁹⁸ As fluorescence responses falling outside the range of the standard curve cannot be assigned specific concentration values and can only be extrapolated, these values are denoted as out of range. For comparison purposes, we work directly with detected fluorescence responses rather than converting them to concentration values. This approach is beneficial because fluorescence can detect low signals without needing to assign an appropriate level of detection, making it more effective for testing differences in analyte expression.⁹⁸

Experimental groups were compared using a moderated t-test via the limma package,⁹⁹ and corrected using Benjamini-Hochberg (BH) method to modulate false discovery rate.¹⁰⁰ An adjusted *p*-value of < 0.05 was considered statistically significant. The results were visualized using GraphPad Prism (version 10.0.3).

4.0 RESULTS

4.1 Interaction analysis of AdV-based vaccines and PF4

4.1.1 Biolayer interferometry (BLI)

The interaction between PF4 and AdV-based vaccines was first assessed using BLI, with bPF4 acting as the ligand (Figure 1). For binding experiments, increasing concentrations of bPF4 were immobilized onto streptavidin sensors to determine its association with the AdV-based vaccines. The stock concentrations of the vaccines were used, allowing for the detection of the highest PF4 binding signal if such an interaction exists. However, no interaction was observed between

PF4 and any of the vaccines at any bPF4 concentrations. Even at the highest concentration of PF4 used (2500 nM), the binding response between PF4 and ChAdOx1-S was 0.4129 nm, and for Ad26.COv2.S, it was less than 0 nm, indicating continued dissociation of bPF4. These binding responses are negligible compared to the positive control of polyclonal anti-PF4, which shows a binding response of 2.36 nm at the K_D of 97.42 nM (Figure 2). However, they are comparable to the negative control of anti-hexon, which targets the adenoviral hexon capsid protein and showed a response of 0.1526 nm at 750 nM of immobilized bPF4.

For the inversed setup with PF4 serves as the analyte, activated amine coupling sensors are intended to be loaded with AdV-based vaccines to interact with increasing concentrations of PF4 (Figure 3). Unlike the previous setup, where the vaccines did not exhibit detectable background binding to the streptavidin sensor, PF4 showed a prominent affinity to the amine coupling sensor surface with a binding response of 1.533 nm. This substantial nonspecific binding overshadowed any potential interaction between PF4 and ChAdOx1-S, which showed a binding response of 1.506 nm.

4.1.2 Surface plasmon resonance (SPR)

The interaction between PF4 and AdV-based vaccines was then assessed using SPR, with bPF4 acting as the ligand (Figure 4). For binding experiments, bPF4 were immobilized onto streptavidin-coated CM4 sensors to determine its association with increasing concentrations of AdV-based vaccines. These binding

responses were then normalized to account for the background interactions between the vaccines and the streptavidin-coated sensor surface.

Prior to normalization, we observed high interactions between the three vaccines and immobilized bPF4, with interaction responses increasing with rising vaccine concentrations. (Supplementary Figures 1 – 3). The bPF4 binding responses were 463.2 RU for ChAdOx1-S, 3054 RU for Ad26.COVS2.S, and 2979 RU for Ad26.ZIKV at 4.8×10^{10} VP/mL. However, we also found prominent background interactions between all three vaccines and the streptavidin-coated CM4 chip, with binding responses reaching 1116 RU for ChAdOx1-S, 3035 RU for Ad26.COVS2.S, and 2963 RU for Ad26.ZIKV at 4.8×10^{10} VP/mL (Supplementary Figures 1 – 3). Notably, the background interaction between ChAdOx1-S and the streptavidin-coated CM4 chip surface was higher than its interaction with bPF4. Therefore, after normalizing for background binding, ChAdOx1-S displayed increasingly negative interaction responses with rising vaccine concentrations, while Ad26.COVS2.S and Ad26.ZIKV showed minimal interaction responses of 12.44 RU and 11.09 RU at their respective K_D , or EC50 values.

These binding observed between bPF4 and the Ad26-based vaccines were minimal compared to the positive control of anti-PF4 antibodies to immobilized bPF4, which showed an EC50 value of 102.3 RU after normalizing for background binding to the streptavidin-coated sensor surface (Figure 5). However, these values were higher than the negative control of anti-hexon to immobilized bPF4, which showed a binding response of less than 1 RU (Figure 5).

Next, PF4 was used as the analyte to measure its association with sensor-immobilized AdV-based vaccines (Figure 6). For binding experiments, the vaccines

were immobilized onto anti-hexon coated C1 sensors to determine their association with increasing concentrations of PF4. These binding responses have been normalized to account for the background interaction between PF4 and the anti-hexon-coated sensor surface.

We observed high binding responses between PF4 and all three vaccines, with EC50 values of 670.5 RU, 625.5 RU, and 376.7 RU for ChAdOx1-S, Ad26.COVS2.S, and Ad26.ZIKV, respectively. While the interaction between immobilized anti-PF4 and PF4 exhibited an EC50 of 60.0 RU, these PF4/vaccine binding responses exceeded that of the positive control by several folds (Figure 7).

Despite the overall high binding responses, all three vaccines exhibited lower binding affinity than the positive control anti-PF4 to PF4 interaction. The K_D for anti-PF4 to PF4 was 197.5 nM, whereas ChAdOx1-S, Ad26.COVS2.S, and Ad26.ZIKV exhibited K_D of 272.1 nM, 308.2 nM, and 259.4 nM, respectively. Notably, PF4 also exhibited a high binding response to the immobilized anti-hexon (439.7 RU), which serves as a negative control, though the binding affinity was relatively low ($K_D = 966.9$ nM).

To highlight the sensitivity differences between SPR and BLI, we adapted the SPR experimental setup for BLI to evaluate whether BLI could detect small molecular binding (anti-hexon) after capturing a much larger molecule (ChAdOx1-S). The specificity of anti-hexon for ChAdOx1-S was confirmed by a loading response of 1.476 nm when ChAdOx1-S was loaded onto the sensor-immobilized anti-hexon (Supplementary Figure 4). However, a minimal binding response shift of 0.0913 nm was observed during anti-hexon enrichment with the captured ChAdOx1-S, indicating that only background binding activity was detectable.

4.2 Cytokine profiling

4.2.1 No significant association between cytokine levels and VITT antibodies development

We investigated the association between cytokine levels and the development of VITT antibodies. This was done by comparing the serum cytokine levels of two patient cohorts suspected of VITT following AdV-based vaccination: those serologically diagnosed with anti-PF4 antibodies (VITTpos) and those without (VITTneg) (Figure 9).

Our analysis found no significant association between cytokine levels and the development of VITT antibodies, as none of the tested cytokines exhibited significant differences between the VITTpos and VITTneg cohorts.

However, although not statistically significant, two cytokines showed notable variation between the two cohorts. Specifically, IL-6 level was elevated in the VITTneg compared to VITTpos cohort, with median levels of 575.8 FI and 140 FI, respectively. This elevation is approaching statistical significance ($p = 0.056$).

Conversely, although the median IL-10 levels were similar between the VITTpos and VITTneg patients (75.5 FI and 78.5 FI, respectively), the VITTpos cohort exhibited a broad distribution of IL-10 levels compared to the VITTneg cohort, with ranges of 11 – 592 FI for VITTpos and 31-146.5 FI for VITTneg.

4.2.2 HIT patients exhibit an elevated inflammatory state compared to VITT patients

Given the similar clinical characteristics of VITT and HIT, and that both disorders are mediated by anti-PF4 antibodies, we explored whether the cytokine

profiles of VITT and HIT patients share common features. This investigation aimed to determine if the development of pathogenic antibodies in anti-PF4 antibody-mediated disorders occurs within a similar cytokine environment.

To evaluate this, we compared the serum cytokine levels of patients diagnosed with VITT (VITTpos) and HIT (HITpos), based on the presence of platelet-activating anti-PF4 antibodies (Figure 10). Our analysis revealed significant differences in the cytokine profiles between the two cohorts. Specifically, the HITpos cohort showed significantly higher levels of inflammatory cytokines, including eotaxin ($p = 0.037$), IL-6 ($p = 0.003$), IL-8 ($p = 0.007$), IL-15 ($p = 0.031$), IL-18 ($p = 0.0009$), IL-27 ($p = 0.04$), IP-10 ($p = 6.56E-07$), MIG ($p = 0.037$), sCD40L ($p = 0.002$), and regulatory cytokines IL-1RA ($p = 0.031$) and IL-10 ($p = 0.025$), compared to the VITTpos cohort.

4.2.3 VITT disease severity correlates with a heightened inflammatory state

As VITT patients with CVST exhibit the highest mortality rate among all VITT patients, we selected VITT patients with CVST to represent those with the most severe disease manifestations. Therefore, we compared the cytokine levels between two cohorts serologically diagnosed with platelet-activating anti-PF4 antibodies: VITT-positive patients with CVST (VITTpos_CVST) and those with thrombotic events in other sites (VITTpos_other) (Figure 8). Our goal was to investigate whether an elevated proinflammatory cytokine environment is more prevalent in VITT patients with CVST compared to those without it, thereby associating this elevated inflammation with the severity of VITT.

Analysis revealed that IL-8 levels were significantly elevated in the VITTpos_CVST cohort compared to the VITTpos_other cohort ($p = 0.0003$), with median IL-8 levels of 216 FI and 49 FI, respectively. This indicates a heightened proinflammatory state in the most severely affected VITT patients.

Conversely, although IL-6 levels were also consistently elevated in VTE,^{74,75} there were no statistically significant differences in IL-6 levels between the two cohorts ($p = 0.946$), with median levels of 232 FI and 120.5 FI, respectively. Moreover, IL-6 levels exhibited a wide distribution across both patient cohorts, with ranges of 24.5 – 695.5 FI in the VITTpos_CVST cohort and 36.5 – 767.5 FI in the VITTpos_other cohort. These results indicate considerable variability in the inflammatory response among VITT patients.

5.0 DISCUSSION

VITT is a rare, life-threatening thrombotic disorder observed following administration of ChAdOx1-S and Ad26.COV2.S AdV-based SARS-CoV-2 vaccines. It is characterized by thrombocytopenia accompanied by thrombosis at various sites, with notably high incidences of CVST and SVT.^{18,67} The pathogenic mechanism of VITT involves anti-PF4 antibodies that can activate platelets via FcγRIIa-mediated signalling in the presence of PF4 and initiate thrombi development.⁶¹ The genesis of these pathogenic anti-PF4 antibodies is hypothesized to mimic HIT; another drug mediated disorder with a heightened risk of thrombosis, wherein a polyanionic molecule (such as the anticoagulant heparin) forms immune complexes with PF4, triggering antibody production.⁶⁸ In VITT, the electronegatively charged AdV molecules are proposed to bind PF4, forming

similar immune complexes as PF4/heparin.⁶⁸ In addition to the PF4/AdV immunogen, vaccine excipients are implicated in creating an inflammatory environment conducive to antibody formation.^{67,69} However, conflicting evidence were presented regarding both theories.^{57,69} Some question the binding capability of PF4 with vaccine particles,⁶⁹ while others highlight that vaccine excipients are unlikely to present at the time symptoms appear.⁵⁷ This raises doubts about the actual contribution of PF4/AdV complexes and excipient-induced inflammatory conditions to anti-PF4 antibody formation.

Given the mounting conflicting evidence against both theories, this study aims to consolidate the binding interactions between PF4 and AdV-based vaccines using two optical techniques to evaluate their potential for complex formation. Additionally, we investigated whether cytokines contribute to an inflammatory environment that correlates with disease severity and the formation of anti-PF4 antibodies in VITT.

As the use of AdV-based therapies continues to expand, it is crucial to address their potential induction of thrombotic conditions like VITT. Beyond SARS-CoV-2 vaccination, AdV platforms have been used in various therapeutic applications due to their high transduction efficiency for diverse host cell types, large packaging capacity for genetic material, and non-integration into the host genome.³⁰ These advantages have made AdV valuable in gene therapy, cancer treatment, and vaccines against infectious diseases such as Ebola, human immunodeficiency virus, and malaria.³⁰ Additionally, their lower manufacturing costs and stability at higher temperatures make them more accessible to developing

countries, which often lack the financial resources and ultralow temperature storage facilities required for mRNA vaccines.^{30,101}

Therefore, understanding their potential interactions to endogenous proteins like PF4 and the immune responses triggered by AdV-based vaccination is essential for preventing thrombotic consequences associated with these therapeutic applications.

5.1 Interaction analysis between PF4 and AdV-based vaccines

5.1.1 BLI is unsuitable for illustrating reversible binding between PF4 and AdV-based vaccines

In experiments where bPF4 served as the ligand, we immobilized increasing concentrations of bPF4 on streptavidin-coated BLI sensors and tested its association with the AdV-based vaccines. We found no significant interaction between PF4 and any of the ChAdOx1-S, Ad26.COV2.S, or Ad26.ZIKV vaccines, with the interaction response aligning with that of the negative control of anti-hexon antibodies (Figure 1). Additionally, there was no background interaction between the vaccines and the streptavidin sensor surface, indicating that the lack of binding was not due to background interference masking the true PF4/AdV interaction. These results suggest that bPF4 does not bind to these vaccines under the tested conditions in BLI. However, considering the small molecular weight of PF4 (31.2 kDa), a potential issue arises. The biotinylation process, even with the use of a medium-length spacer arm sulfo-NHS-LC-biotin,⁶⁵ may have disrupted PF4's critical binding sites with the AdV-based vaccines, which could potentially explain the absence of observed interaction.

Ideally, to confirm the lack of interaction observed when using bPF4 as a ligand, the vaccine particles should be biotinylated and immobilized on streptavidin sensors to use PF4 as an analyte for interaction measurements. However, due to limited vaccine volumes, we were unable to perform biotinylation on the vaccines. We instead used amine coupling sensors, which allowed us to immobilize the vaccines directly onto the sensors. This approach aimed to preserve the integrity of the binding sites and provide a more direct measurement of the interactions between PF4 and the AdV-based vaccines.

Using amine coupling sensors, the vaccines were immobilized on the sensors to test their association with non-biotinylated PF4 acting as the analyte. In this setup, although binding was detected between ChAdOx1-S and PF4, we observed even higher background binding between PF4 and the amine coupling sensor surface. This significant background interaction likely masked the true PF4/AdV interaction response, if one exists, thereby undermining the reliability of the assay in accurately assessing the specific interactions. Moreover, if substantial binding between PF4 and ChAdOx1-S did exist, it would likely be more pronounced than the background interaction observed. Consequently, the use of amine coupling sensors proved unsuitable for accurately measuring interactions between PF4 and AdV-based vaccines, raising questions about the underlying causes of the observed background binding.

This prominent interaction between PF4 and the amine coupling sensor was unexpected, given that the sensor surface should remain neutral throughout the cross-coupling process, theoretically preventing electrostatic interaction with the cationic PF4. For amine coupling sensors, cross-coupling is achieved by activating

the sensor's surface-coated carboxyl groups. Activation through s-NHS and EDC forms reactive NHS ester intermediates that facilitate the crosslinking with primary amine groups on the ligand. At physiological pH, these intermediates do not ionize and should be neutrally charged. After quenching with ethanolamine to block any remaining unreacted sites, the resulting amide product on the sensor surface should also remain neutrally charged (Supplementary Figure 2). This neutrality would theoretically prevent electrostatic interactions between PF4 and the quenched groups, or any remaining unquenched groups, on the sensor surface. However, beyond this equatorial ring of cationic amino acids, there are various amino acids distributed around the surface of PF4 capable of forming hydrogen bonds with the hydroxyl or amide groups on the quenched molecule. These residues include the amide groups of asparagine and glutamine, as well as the hydroxyl groups of serine and threonine.¹⁰² Nevertheless, the binding of PF4 to the amine coupling surface suggests a propensity for PF4 to interact with chemical groups during the amine-coupling process, warranting further investigations.

Although PF4 showed no binding to AdV when acting as a ligand, its high background interaction with the amine sensor surface when acting as an analyte question whether BLI can consistently detect true PF4/AdV binding. These findings suggest that alternative experimental techniques may be necessary to accurately evaluate these interactions.

5.1.2 SPR demonstrated binding only between PF4 and the Ad26-based vaccines when bPF4 acts as the ligand

We used SPR to further explore the interaction between PF4 and AdV-based vaccines. SPR employs a continuous flow system, which reduces mass transport limitations and offers greater sensitivity than BLI, especially for interactions with low molecular weight molecules. In contrast, the lack of a flow system in BLI can lead to sample evaporation and drifts in interaction curves, as immobilized ligands cannot be constantly exposed to fresh analyte, resulting in reduced sensitivity.⁹⁵ Published literature reports the sensitivity of SPR and BLI to reach 0.01 pg/mm² and 10 pg/mm², respectively, indicating that SPR is capable of detecting much smaller changes in mass per square millimeter of the sensor surface.¹⁰³

With bPF4 acting as the ligand using a streptavidin-coated CM4 sensor, we found positive binding responses between PF4 and both Ad26-based vaccines (Ad26.COVS and Ad26.ZIKV), but not with ChAdOx1-S (Figure 3). The lack of interaction observed between PF4 and ChAdOx1-S is likely due to its high background interaction with the reference cell containing a biotin-coated streptavidin surface (Supplementary Figure 1). Specifically, ChAdOx1-S appears to have a higher affinity for the sensor surface compared to bPF4, as the binding response to bPF4 becomes increasingly negative with rising ChAdOx1-S concentrations. Moreover, although we observed a positive binding response that increased with rising concentrations of Ad26-based vaccines, these vaccines also exhibited significant background binding to the sensor surface.

These differences in binding profiles of ChAdOx1 and Ad26-based vaccines to the sensor surface stem from the unique sequences of the AdV protein

components, including fiber, hexon, and penton proteins, classified based on their serotype.¹⁰⁴ The hypervariable regions (HVRs) within these proteins influence their interaction with host cells and other biomolecules.^{105,106} Hexon proteins, the most abundant part of the adenovirus capsid, feature HVRs that help evade neutralizing antibodies generated from previous infections or vaccinations by altering antigenic sequences.^{105,106} Conversely, penton and fiber proteins facilitate viral attachment to host receptors, which vary across different cell types and serotypes.¹⁰⁷ Thus, the variability in surface chemistry among serotypes significantly affects their biomolecular interactions, including those with bPF4 and the sensor surface, resulting in the varied binding profiles observed in experiments with ChAdOx1-S versus Ad26-based vaccines. However, we cannot rule out the possibility that certain excipients in the vaccine preparations, differing between ChAdOx1-based and Ad26-based vaccines, may also contribute to the interactions observed with the sensor surface.

As none of the vaccines exhibited binding to the streptavidin sensor surface in BLI, the high background interaction observed with the CM4 chip may be attributed to its dextran coating, suggesting that CM4 sensor chip is not suitable for measuring interactions between PF4 and AdV-based vaccines. Dextran is a three-dimensional network of polysaccharide chains, which significantly increases the surface area available for ligand immobilization, allowing for a higher density of immobilized molecules and enhancing the sensitivity of the SPR assay. The dextran itself does not impart an overall charge to the molecule, making it unlikely to participate in electrostatic interactions with the vaccines. However, due to its hydrophilic nature, dextran may form hydrogen bonds with surface proteins on the

adenoviral capsid, potentially creating background interactions with the vaccines. Therefore, a different type of sensor chip without a dextran layer is needed to accurately measure the interactions between PF4 and AdV-based vaccines in SPR.

5.1.3 SPR demonstrated binding between PF4 and all three vaccines when PF4 is used as the analyte

Given that the dextran layer likely induced high hydrophilic background binding on the CM4 chip, we employed a C1 chip that lacks a dextran layer to mitigate this issue. In this setup, PF4 served as the analyte to interact with AdV-based vaccines captured on the sensor via sensor-immobilized anti-hexon antibodies. Significant PF4 binding was observed across all three AdV-based vaccines. Specifically, the SARS-CoV-2 vaccines (ChAdOx1-S and Ad26.COVS2.S) demonstrated higher EC50 binding response at K_D values compared to Ad26.ZIKV, with ChAdOx1-S exhibiting higher binding affinities than Ad26.COVS2.S. These results correlate with the differing incidence rates of VITT, with ChAdOx1-S inducing the highest rates.^{19,20}

Notably, the SARS-CoV-2 vaccines exhibited more than a 20-fold higher EC50 despite a 1.5-fold lower binding affinity compared to the positive control (anti-PF4). This discrepancy suggests that while the strength of individual binding events does not surpass that of antigen-antibody interactions, the overall PF4/AdV interaction is extensive. Previous studies have demonstrated that PF4 can bind to multiple sites within the interhexon spaces, located between either two or three hexons, on the adenoviral capsids of both ChAdOx1 and Ad26.⁶⁸ Therefore, each vaccine particle functions as a multivalent ligand with a large surface area, capable

of interacting with numerous PF4 molecules. This multivalent nature results in a higher perceived binding response compared to anti-PF4, which has only two analyte binding sites. Additionally, the simultaneous binding of multiple PF4 molecules makes it unlikely that all will dissociate at once, resulting in a stronger overall measured interaction, even if the individual interactions are weaker. Consequently, despite showing only a 1.5x lower binding affinity compared to the anti-PF4 positive control, the individual interactions between PF4 and the vaccines are likely weaker, though this cannot be fully validated with our current experiment, as only avidity was measured. Despite the high perceived binding, however, further investigation is needed to determine whether these PF4/AdV complexes alone can trigger an immune response strong enough to induce antibody production under physiological conditions.

Our findings are consistent with those of Baker *et al.*, demonstrating interactions between both ChAdOx1 and Ad26-based vaccines with PF4.⁶⁸ However, the binding responses we observed were significantly higher than those reported in the published literature.⁶⁸ This substantial binding may be attributed to differences in our experimental setup. Specifically, the use of anti-hexon antibodies to capture viral vectors in our experiment likely increased the exposed surface area of the viral particles, allowing for more extensive interactions with PF4. As SPR measures the mass of bound molecules, this extensive interaction with the large exposed AdV surface area can lead to a significant increase in the overall RU detected, resulting in a higher apparent binding response. In contrast to our anti-hexon capturing method, which provides an assessment of the specific interaction between PF4 and the vaccine viral particles, Baker *et al.* immobilized the entire

vaccine preparation, including excipients, directly onto the sensor chip via amine coupling. This approach could introduce confounding factors onto the chip surface, potentially reducing the number of viral particles immobilized and, consequently, the binding response with PF4. This is especially relevant for ChAdOx1-S, given the substantial amounts of production-related host cell proteins and significant variability in impurity concentrations across batches.^{69,70} However, it is important to note that we cannot rule out the possibility that the anti-PF4 immunogen may form through interactions between PF4 and vaccine excipients. Further investigation is needed to fully understand the role of vaccine components in PF4 interactions and VITT pathogenesis.

On the other hand, the higher PF4 binding with the Ad26.COVS2 compared to Ad26.ZIKV imply that specific vaccine excipients or features of the vaccine particles themselves contribute to the interaction with PF4. Given that no studies have investigated the levels of production-related impurities in Ad26.ZIKV, we are unable to determine whether differences in impurity levels correlate with the variability in PF4 binding. Unique components of each vaccine, however, such as the expression of the inserted gene on the vector surface, may also play a role in the observed interaction differences. These unique antigens or structural features specific to each vaccine formulation should be further investigated for their potential contribution to PF4 binding, as they could influence the vaccine's immunogenic profile and its interaction with PF4. Therefore, understanding the surface chemistry between different Ad serotypes as well as the unique components within each vaccine are essential for designing AdV-based therapies that minimize unintended interactions, thus reducing the risk of adverse events such as VITT.

However, a limitation is that the vaccine viral particles were not purified from the vaccine preparations. Therefore, the binding observed might be between PF4 and the anti-hexon captured viral particles or free hexons, with the amount of free hexon captured depending on their concentration in each vaccine. Consequently, we cannot rule out that the differences in binding response observed between the vaccines are due to variations in free hexon concentrations in these vaccine preparations. Moreover, since Ad26.ZIKV has not been linked to any VITT cases, it suggests there may be a threshold of PF4 interaction that does not trigger immune activation. However, whether the PF4/Ad26.ZIKV interaction should be considered the true negative control for these experiments requires further investigation.

Interestingly, we also observed PF4 interacting with the negative control (anti-hexon). Compared to the positive control (anti-PF4), PF4 binding to anti-hexon exhibited an EC₅₀ more than 8-fold higher, while the binding affinity was 4.8-fold lower. As hexon is the targeted analyte of anti-hexon, the binding of PF4 to anti-hexon could suggest a structural similarity between PF4 and hexon, resulting in a cross-reactivity between PF4 and anti-hexon. However, given the high K_D , this interaction is neither stable nor specific, resulting in a transient interaction. This potential structural similarity between PF4 and hexon warrants further investigation to understand its implications in VITT antibody development, such that whether anti-hexon antibodies produced by AdV-based vaccine recipients can cross-react with endogenous PF4 under physiological conditions. Such cross-reactivity may create a platform for antibody development against PF4, potentially facilitated by the formation of PF4/AdV complexes.

While this interaction is clearly detected in SPR, potential reasons for its absence in BLI may involve both the experimental setup and the inherent sensitivity limitations of BLI. Brownian dynamics simulations demonstrated that PF4 frequently contacts the AdV capsid surface, especially between hexons, where negative charge is concentrated.⁶⁸ This interaction is driven by both electrostatic and shape complementarity, allowing PF4 to "sink" into the interhexon space, stabilizing the interaction within the socket-like structure.⁶⁸ When using BLI with biotinylated PF4 immobilized to associate with the vaccines, PF4 is restricted from freely rolling on the surface and can only bind to one face of the AdV particle. This restricts PF4 from accessing the interhexon spaces and fully coating the AdV surface, as it is able to do in the current SPR setup, thereby limiting its interaction with the viral particles and resulting in a significantly lower binding response.

On the other hand, we cannot fully replicate the current SPR setup using BLI to determine if the interaction is detectable via the same experimental setup. We previously demonstrated that BLI is unable to effectively distinguish between PF4's background binding to the amine coupling sensor and its binding to AdV, which prevents us from using PF4 as the analyte on BLI sensors. To further demonstrate BLI's sensitivity limitations, we adapted the current SPR setup for BLI, substituting anti-hexon for PF4 as the analyte. This approach allowed us to evaluate whether BLI could detect the binding of a small molecule, in this case, the positive control anti-hexon, after the significantly larger AdV molecule had already been bound to the sensor. We found that while ChAdOx1-S loading to immobilized anti-hexon produced a strong response of 1.476 nm, confirming specific interaction, the secondary signal from the anti-hexon analyte showed minimal binding at 0.0913

nm (Supplementary Figure 2). This minimal signal suggests that BLI loses sensitivity in detecting smaller molecules after a larger one is bound. In contrast, SPR maintained high sensitivity and a strong binding response under the same conditions, highlighting the sensitivity limitations of BLI in this context.

5.1.3 Limitations

One consideration in these interaction analyses is that specific plasma PF4 concentrations during the acute phase of VITT have not been thoroughly investigated in previous literature. The PF4 concentrations used in our study mimic those employed in the experiments by *Baker et al.*, which aimed to establish binding during a hyperinflammatory phase with extensive platelet activation. Although the K_D values of PF4 to vaccine binding determined by SPR fall within the PF4 concentration range we used, suggesting the possibility of PF4/AdV complexes acting as immunogens for anti-PF4 development, it remains unknown whether plasma PF4 concentrations following vaccination can reach such levels. Therefore, further investigation is needed to determine if stable complex formation can occur for the vaccines under physiological conditions, specifically focusing on plasma PF4 concentrations during the acute phase of VITT.

5.2 Cytokine profiling of VITT patients

5.2.1 No significant correlations found between cytokine levels and antibody production in VITT

We compared cytokine profiles between suspected VITT patients who were serologically diagnosed with VITT by the presence of platelet-activating anti-PF4 antibodies (VITTpos) and those without these antibodies (VITTneg) to explore the

relationship between cytokine levels and VITT anti-PF4 antibody development. Our analysis did not reveal statistically significant differences in the levels of any cytokines tested between these cohorts ($p > 0.05$). Therefore, despite the presence of anti-PF4 antibodies, there is a lack of significant differences in B cell activating cytokines between the two cohorts. Although cytokines are essential for antibody production, their involvement in the development of VITT anti-PF4 antibodies was not detectable in our current patient cohorts. Alternatively, the relevant cytokines may not have been included in the panel of cytokines we tested in this study.

Another possibility for the lack of cytokine differences is that both cohorts are experiencing elevated levels of B-cell stimulating cytokines and exhibit antibody development, but with antibodies directed against different antigens. This could result from a pan-cellular activation of B cells caused by the vaccination-induced inflammatory state, driving the development of anti-PF4 antibodies in VITT patients, while inducing antibodies with other antigen specificities in VITTneg patients. Given that VITT is a subset of thrombotic thrombocytopenia syndrome following vaccination, classified based on the presence of anti-PF4 antibodies,¹² VITTneg patients are categorized as VITT-negative based solely due to the absence of anti-PF4 antibodies. Since antibodies against antigens other than PF4 are not tested in suspected VITT patients, this classification does not exclude the presence of other immune-mediated antibodies that could contribute to thrombotic events in VITTneg patients. Further investigations are necessary to explore the involvement of a broader spectrum of antibodies with different antigen specificities in suspected VITT patients to better understand the immune

mechanisms underlying thrombotic complications following AdV-based vaccination.

Although not statistically significant, the variation in IL-6 and IL-10 distributions between the VITTpos and VITTneg cohorts, could offer insights into the differing pathogenic mechanisms underlying the two conditions. Specifically, we observed higher median levels of IL-6 in the VITTneg cohort, with this elevation approaching statistical significance ($p = 0.056$). In contrast, the VITTpos cohort exhibited a broad distribution of IL-10 levels, with both the maximum and minimum value extending four times beyond those of the VITTneg cohort.

IL-6 is produced by various immune and non-immune cells during the acute phase response to infection or tissue injury.¹⁰⁸ It contributes to an inflammatory, procoagulant state by inducing cytotoxic T-cell activation, enhancing vascular permeability and angiogenesis, and promoting monocyte tissue factor expression.¹⁰⁸ Previous studies have established IL-6 as a biomarker for viral infections, with significantly elevated levels observed in natural adenoviral infections and AdV-based vaccinations,^{82,83,109} including those using Ad26 and chimpanzee AdV serotype 155-based vectors.^{82,83} This heightened IL-6 response in VITTneg individuals indicates an inflammatory environment unique to these patients, potentially correlating with thrombus formation.

Interestingly, the VITTneg cohort shares IL-6 elevation with another antibody-mediated thrombotic disorder known as MGUS (Monoclonal Gammopathy of Undetermined Significance).¹¹⁰ MGUS is characterized by the clonal proliferation of monoclonal plasma cells that produce persistent pathogenic antibodies.¹¹¹ These antibodies can trigger recurrent thrombosis and are associated

with a chronic inflammatory state,¹¹² with IgG and IgA MGUS being linked to thrombotic events in both the arterial and venous systems.¹¹³ Recent reports have identified VITT-like platelet-activating anti-PF4 antibodies in two MGUS patients,¹¹⁴⁻¹¹⁶ resulting in recurrent thrombosis and thrombocytopenia without prior heparin exposure.¹¹⁴⁻¹¹⁶ Although the underlying factors that trigger the development of MGUS antibodies are not fully understood, a state of pancellular activation induced by vaccination could potentially activate pre-existing MGUS B cell clone in vaccinated individuals. Depending on the antigen specificity of the B cell, this activation could lead to the production of pro-thrombotic antibodies that are not necessarily PF4-specific. However, while MGUS antibodies are associated with an increased risk of thrombosis,¹¹² the percentage of patients who actually develop thrombosis is relatively low (8% in a three-year period).¹¹⁷ Whether AdV-based vaccinations can induce B cell activation in a broader population but only cause thrombosis in certain individuals with an exaggerated reaction—such as VITTneg patients with elevated IL-6 levels—remains to be investigated.

On the other hand, the implications of the varied IL-10 levels among VITTpos patients are more complex. IL-10 functions in a context-dependent manner, exhibiting both protective and pathogenic effects.¹¹⁸ Primarily known for its ability to suppress excessive pro-inflammatory responses, IL-10 helps mitigate tissue damage and maintain tissue homeostasis.¹¹⁸ Paradoxically, elevated IL-10 levels are associated with increased autoantibody production in certain conditions, though the exact mechanisms are not fully understood.¹¹⁸ Dysregulation of IL-10 has been implicated in the pathology of multiple antibody-mediated autoimmune disorders, including HIT and MGUS.^{78,119}

Our lab has previously demonstrated that HIT patients produce significantly lower levels of IL-10 compared to healthy controls.⁷⁸ This aligns with findings from Pouplard *et al.*, who identified gene polymorphisms in the IL-10 promoter that result in lower IL-10 production in HIT patients,¹²⁰ potentially contributing to HIT immunogenesis by failing to adequately regulate the pro-inflammatory immune response.¹²⁰ Conversely, elevated IL-10 levels have been linked to the disease progression of MGUS.¹¹⁹ Abnormal MGUS plasma cells may progress to malignant multiple myeloma (MM) if they continue to proliferate excessively.¹²¹ Serum IL-10 levels in healthy controls are significantly lower than in MGUS patients, while MGUS patients have lower IL-10 levels than MM patients.¹¹⁹ This suggests a potential role for IL-10 in the progression from MGUS to MM, promoting the proliferation of the malignant plasma cell.^{119,121} Given that both elevation and reduction of IL-10 levels have been linked to immune dysregulation and pathology in various autoimmune disorders, the large variation in IL-10 levels among VITTPos patients may indicate a loss of regulatory control. This dysregulation results in individual differences in IL-10 responses despite being induced by the same pathogenic antibody. Consequently, depending on individual IL-10 levels, it may either promote anti-PF4 antibody development and facilitate plasma cell proliferation or lead to an uncontrolled heightened inflammatory state, both contributing to thrombus formation.

This cytokine pattern of broad IL-10 level distribution versus elevated IL-6 levels reveals distinct inflammatory and regulatory processes in the VITTPos and VITTNeg cohort, suggesting that the pathogenetic mechanisms leading to thrombosis may differ between the cohorts in ways that extend beyond the mere

presence or absence of anti-PF4 antibodies. Whether widespread cellular activation is involved in the immune responses following vaccination, contributing to these varied conditions, would require further investigation.

5.2.2 VITT and HIT anti-PF4 antibodies are associated with distinct cytokine profiles

We next compared the cytokine profiles of patients serologically diagnosed with VITT (VITTpos) and HIT (HITpos). As the pathology of both disorders are mediated by anti-PF4 antibodies, our aim was to determine whether they share similar cytokine profiles, suggesting that anti-PF4 antibody development in both conditions may be influenced by comparable cytokine environments.

Our analysis found significantly elevated levels of several inflammatory cytokines in HITpos patients, suggesting that the heightened inflammatory state observed may be linked to their condition and the presence of HIT-specific anti-PF4 antibodies. Although VITT and HIT share clinical features including thrombocytopenia and potential thrombosis, the nature and extent of these conditions differ. VITT patients exhibit a tendency toward SVT and CVST, with 95% likelihood of developing thrombosis, while HIT patients predominantly experience PE and DVT, with a lower thrombotic rate of 35%.¹²² The differing cytokine environments may be linked to their specific anti-PF4 antibodies, potentially shaping these distinct clinical characteristics of these disorders despite their similarities. However, since we lack cytokine data from before the development of anti-PF4 antibodies, the elevated cytokine levels observed may have pre-existed, potentially playing a role in mediating the development of anti-

PF4 antibodies and contributing to the distinct cytokine environments in VITT and HIT. Alternatively, the differences in anti-PF4 antibody-mediated pathologies between these disorders could have led to the observed variations in cytokine profiles.

When examining the specific proinflammatory cytokines significantly elevated in HIT patients, several indicators suggest that HIT may be more skewed toward a TD B cell response compared to VITT. IL-6 and IL-27 both play critical roles in T follicular helper cell differentiation and germinal center formation,^{87,123} while CD40L, expressed on the surface of T helper cells, provides the essential costimulatory signal for B cell activation.⁷⁶ These observations suggest that anti-PF4 antibody formation in HIT may rely more heavily on T-cell involvement than in VITT, pointing to potentially distinct mechanisms underlying anti-PF4 antibody development in these two conditions.

However, it should be noted that sCD40L is produced not only by activated T cells but also by platelets,⁷⁶ hence the severity of thrombocytopenic conditions likely affects the circulating levels of this cytokine. Compared to HIT, which has median platelet counts ranging from 50 - 80×10⁹/L,⁵² VITT is characterized by more severe thrombocytopenia, with median nadir platelet counts around 25×10⁹/L.^{15,17,57} This greater extent of platelet consumption and depletion in VITT patients may further reduce the availability of sCD40L, resulting in lower levels of sCD40L observed. Further investigation is needed to fully understand the nature of these two disorders, potentially by comparing their cytokine profiles to those of well-characterized TI and TD immune responses.

Interestingly, HITpos patients also exhibited significantly higher levels of the regulatory cytokines IL-1RA ($p = 0.031$) and IL-10 ($p = 0.025$) compared to VITpos patients, alongside increased levels of inflammatory cytokines. These elevated regulatory cytokines might be a response to the heightened inflammatory state observed in HIT, rather than a direct reflection of effective immune regulation.

IL-1RA is a receptor antagonist for the IL-1 receptor, regulating inflammatory responses by competing with IL-1 α and IL-1 β for receptor binding without triggering any intracellular signaling.¹²⁴ It is primarily secreted by activated monocytes and neutrophils in response to proinflammatory stimuli, including IL-1, IL-6, and the regulatory cytokine IL-10.¹²⁴ The elevated levels of IL-1RA observed in HIT patients are likely the body's countermeasure to excessive inflammation, serving to mitigate the heightened inflammatory response.

In contrast, as previously noted, our lab identified reduced IL-10 production in HIT patients compared to healthy individuals.⁷⁸ Specifically, we observed that peripheral blood mononuclear cells (PBMCs) from HIT patients, when stimulated with PF4-heparin complexes, produced lower levels of IL-10 than PBMCs from healthy controls.⁷⁸ Instead of focusing on cytokine production by PBMCs in response to stimulation, this study directly measured cytokine levels in patient sera. Serum cytokine levels can vary significantly from those produced by PBMCs in controlled conditions, reflecting the difference between circulating cytokine concentrations and the cellular capacity to produce cytokines.¹²⁵ One contributing factor to this difference is the production of IL-10 by various cells beyond mononuclear cells, including granulocytes such as mast cells and neutrophils.¹¹⁸ The elevated IL-10 levels observed in HIT serum may suggest a broader regulatory

mechanism at play, with contributions from multiple cell types involved in immune modulation.

However, it is also important to consider the distinct pre-existing cytokine environments in VITT and HIT patients prior to their exposure to AdV-based vaccines or heparin. VITT patients are generally healthy individuals who received AdV-based SARS-CoV-2 vaccines, with likely normal baseline levels of inflammatory cytokines before becoming ill. In contrast, HIT patients often receive heparin during hospitalization for surgeries due to their pre-existing health conditions.¹²⁶⁻¹²⁸ These include chronic conditions that are associated with prolonged inflammatory symptoms and elevated baseline levels of proinflammatory cytokines, such as coronary artery disease that requires cardiopulmonary bypass or osteoarthritis necessitating knee replacements.¹²⁶⁻¹²⁸ Additionally, surgeries themselves generate damage-associated molecular patterns from damaged or stressed cells, activating PRRs on immune cells, which further amplifies the release of inflammatory cytokines.¹⁰⁸ Therefore, depending on their individual medical conditions, suspected HIT patients are likely to exhibit varying degrees of elevated proinflammatory cytokines, potentially higher than the baseline levels observed in VITT patients, and unrelated to their anti-PF4 antibody-associated conditions. Without information on these patients' medical conditions prior to developing HIT, we are unable to determine how much of the elevated inflammatory state is due to pre-existing conditions versus being specifically associated with HIT-related anti-PF4 antibodies.

5.2.3 VITT patients with CVST exhibit higher levels of IL-8 compared to those without CVST.

To determine whether a proinflammatory environment is associated with the severity of VITT, we compared VITT patients with CVST (VITT_CVST), who have a 2.7-fold higher risk of mortality among VITT patients,^{15-17,57} to those experiencing thrombosis in other parts of the body (VITT_other). We found significantly elevated levels of IL-8 in the CVST patients, with their median IL-8 expression five-fold higher compared to the other VITT patients ($p = 0.0003$; Figure 8). This observation indicates that CVST is associated with a more inflammatory environment, with IL-8 levels potentially correlating with the severity of VITT and a supportive environment for enhanced B cell response. However, since no cytokines were found to correlate with VITT anti-PF4 antibody production (refer to Section 5.2.1), these findings suggest that while elevated IL-8 may exacerbate disease severity, it does not necessarily play a significant role in the formation of VITT antibodies.

IL-8 is a proinflammatory cytokine produced by various cell types, including neutrophils, monocytes, and endothelial cells,¹²⁹ and is known to be involved in the pathology of VTE.^{74,75} As a potent activator and attractant for neutrophils, IL-8 induces neutrophil activation through a process called NETosis, triggering the release of decondensed DNA coated with histones and various bactericidal proteins known as neutrophil extracellular traps (NETs).¹³⁰ NETosis has been implicated in the pathology of thrombotic conditions, including VITT and HIT,^{67,131,132} due to its pivotal role in thrombus development by trapping platelets and facilitating fibrin deposition.^{133,134} Studies have found that both HIT and VITT

anti-PF4 antibody immune complexes can directly engage with FcγRIIIa receptors on neutrophils, triggering their activation and the release of NETs.^{133,134} Moreover, recent evidence has implicated NETosis in the development of CVST in VITT patients, with high concentrations of NETosis markers found in tissue sections obtained from VITT patients who developed CVST.^{56,67,135} The elevated IL-8 levels observed in VITT_CVST patients in this study further support the involvement of NETosis in thrombus formation at this location. Although it is no longer possible to determine whether the initiation of IL-8 elevation is a cause or consequences of CVST development in these patients, IL-8 released by neutrophils following activation can act in an autocrine fashion, inducing more NETosis and contributing to clot formation.¹³⁶ This process is likely to be more pronounced in an environment with elevated IL-8, highlighting its role in enhancing the pro-thrombotic environment in CVST patients with VITT. Given that CVST is associated with higher mortality and more severe pathology in VITT, the elevated IL-8 levels and increased extent of NETosis aligns with the clinical picture of these patients.

Aside from the involvement of NETosis, Huynh *et al.* identified that VITT antibodies that exhibit a two-site binding profile on PF4 have a stronger association with the occurrence of CVST compared with those that exhibit a single-site binding affinity.¹³⁷ This distinction is evident as patients with two-site affinity antibodies have a much higher incidence rate of CVST (50.0%) than patients with one-site affinity antibodies (5.9%).¹³⁷ Although IL-8 does not play a significant role in directly inducing B cell activation or plasma cell formation, the proinflammatory environment created by elevated IL-8 levels might contribute to the formation of these CVST-related antibodies.

Interestingly, although elevated IL-6 and IL-8 levels have been consistently observed in VTE patients, we did not see this elevation in our VITT_CVST patient cohort. This difference may be specific to CVST versus more common forms of VTE (PE, DVT, and SVT).^{74,75,138} However, a retrospective analysis of CVST inflammatory markers has identified elevated IL-6 levels in CVST patients, with levels positively correlating with disease severity.¹³⁹ The risk factors for CVST in these studies included pregnancy, anemia, and both bacterial and viral infections. These differing findings suggest that CVST development in VITT may involve unique underlying mechanisms characterized by a distinct inflammatory profile.

5.2.4 Limitations

The cytokine study faced several limitations. Firstly, the rarity of VITT samples, particularly those with CVST, led to a small sample size that may not fully represent the entire landscape of these conditions. As VITT is unlikely to reoccur in the foreseeing future with the discontinuation of AdV-based SARS-CoV-2 vaccines, acquiring additional samples is improbable. Specifically, we only obtained samples from one VITTneg patient with CVST compared to ten patients with CVST in the VITTpos cohort. This reflects the clinical reality where CVST occurrence in VITTneg patients is extremely rare, though it results in an unequal distribution in our cohorts.¹⁴⁰

Moreover, without access to the medical records of HIT patients, we are unable to determine their underlying medical conditions and, therefore, cannot fully explain the reasons for their cytokine distribution. Different pre-existing health conditions may influence baseline cytokine levels, making it difficult to discern

whether the elevated cytokine levels are due to HIT or their pre-existing health conditions. Additionally, the small sample size of HIT patients may not be representative of the entire cohort and could include outlier cases that contribute to the elevated inflammatory cytokine levels observed in these patients.

6.0 CONCLUSIONS

In this study, we investigated the interactions between PF4 and AdV-based vaccines, as well as the cytokine profiles of VITT patients. Our focus was on understanding the potential interaction of PF4/AdV-based vaccine complexes in forming the immunogen for VITT anti-PF4 antibodies, and the association of a hyperinflammatory state to VITT severity and antibody production, aiming to elucidate their correlation to the development of VITT pathogenesis.

Of the four experimental setups employed across two optical technologies (BLI, SPR) to measure the interaction between PF4 and AdV-based vaccines, only one setup using the more sensitive technology, SPR, detected this interaction. While the interaction response was substantial compared to the positive control, suggesting the potential for PF4/AdV complex formation following vaccination, this finding was not corroborated by other experimental setups or technologies. Given the higher sensitivity of SPR, the absence of interaction detected in BLI suggests that the interactions between PF4 and AdV-based vaccines are weak. It remains unknown whether additional contributing factors may exacerbate or stabilize this complex formation, enabling this complex to function as an immunogen under physiological conditions.

Further studies are required to validate these interactions using technologies that share similar detection sensitivity, in order to detect the interaction consistently if one exists, across different detection methods. Additionally, employing fluid phase detection methods that do not rely on immobilization can prevent potential blocking of critical molecular interaction sites, thereby providing a more accurate assessment of the interactions.

Our cytokine analysis revealed significantly elevated levels of IL-8 in VITT patients with CVST, suggesting a link between disease severity and an amplified proinflammatory response in these patients. The differences in the cytokine environment between VITT and HIT also suggest that distinct mechanisms may be associated with the specific anti-PF4 antibodies of each disorder, despite their shared clinical characteristics. However, it remains unclear whether the heightened inflammatory state is a contributor to or a consequence of anti-PF4-mediated pathology, or to what extent pre-existing health conditions contribute to the elevated inflammation observed in HIT patients. Moreover, as we found no cytokine correlation with VITT anti-PF4 antibody production, it suggests that while an inflammatory state is correlated with disease severity and supports antibody development, it does not necessarily play a significant role in the formation of anti-PF4 antibodies following AdV-based vaccination. Nonetheless, since cytokines are essential for antibody production, their role in the development of anti-PF4 antibodies may simply not be detectable with the current patient cohorts, warranting further investigation.

Overall, weak interactions exist between PF4 and AdV-based vaccines. Further exploration is needed to determine whether these complexes can act as immunogens for inducing anti-PF4 antibody development under physiological conditions. While an elevated inflammatory state is associated with VITT severity, we did not find a correlation between inflammation and anti-PF4 antibody development in our patient cohorts. Moreover, despite both VITT and HIT being anti-PF4 mediated disorders, they exhibit distinct cytokine environments, which may be linked to the specific conditions and the presence of anti-PF4 antibodies unique to each disorder. Understanding the interactions between AdV-based vaccines and endogenous proteins like PF4, as well as the immune responses triggered by these vaccines, are critical for preventing thrombotic consequences associated with these therapeutic applications and ensuring the continued use of AdV-based therapeutics in the future.

8.0 FIGURES

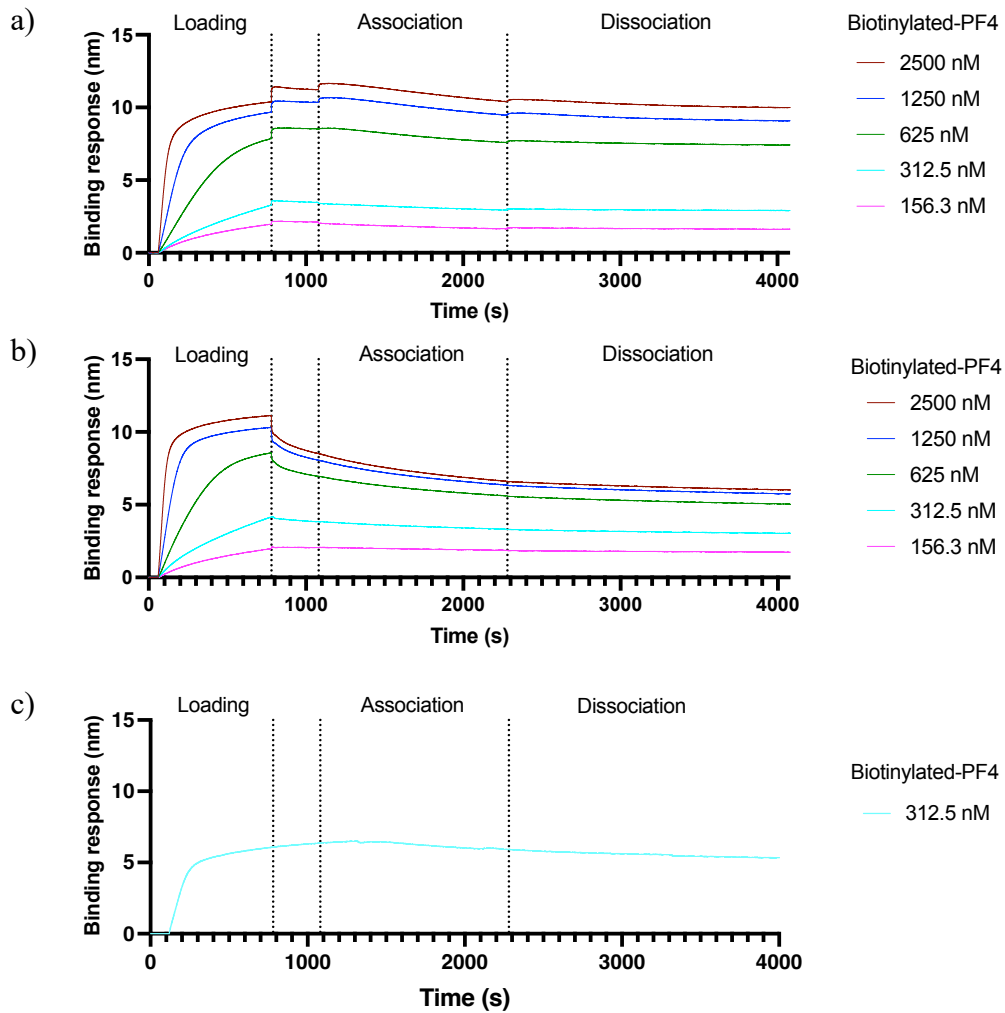


Figure 1. BLI interaction analysis of AdV-based vaccines with immobilized bPF4 using streptavidin sensors. Sensorgrams representing the binding responses of a) ChAdOx1-S, b) Ad26.COVID.S, and c) Ad26.ZIKV against increasing concentrations of bPF4. In each experiment, bPF4 is immobilized on streptavidin sensors for association with the AdV-based vaccines at their respective stock concentrations (ChAdOx1-S: 1.2×10^{12} VP/mL; Ad26-based vaccines: 1.0×10^{11} VP/mL). Due to limited volume, Ad26.ZIKV was used to interact with a single concentration of bPF4 (312.5 nM). The loading of PF4 is shown here to illustrate that binding to the vaccines is absent regardless of ligand concentration. Each vaccine binding experiment was conducted in its respective vaccine buffer. Results have been normalized to their respective reference cell.

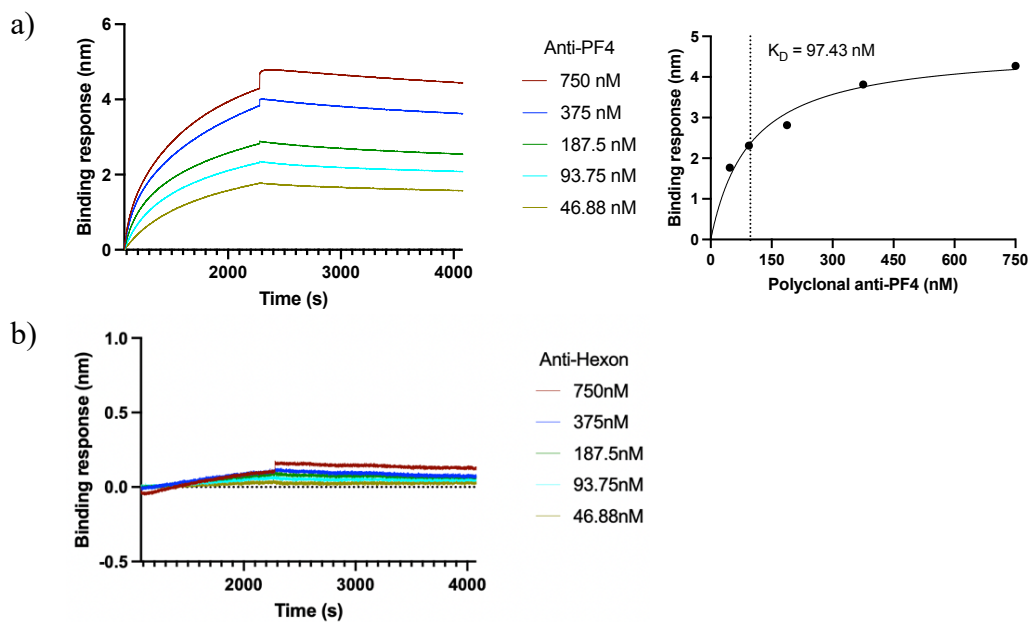


Figure 2. BLI control experiments with immobilized bPF4 using streptavidin sensors. Sensorgrams representing the binding responses of bPF4 against increasing concentrations of a) the positive control polyclonal anti-PF4 and b) the negative control anti-hexon. In each experiment, 10 $\mu\text{g}/\text{mL}$ of bPF4 is immobilized on streptavidin sensors for association with the antibodies. The binding affinity between PF4 and anti-PF4 was calculated using steady-state approximation based on the equilibrium binding response at each antibody concentration. Results have been normalized to their respective reference cell.

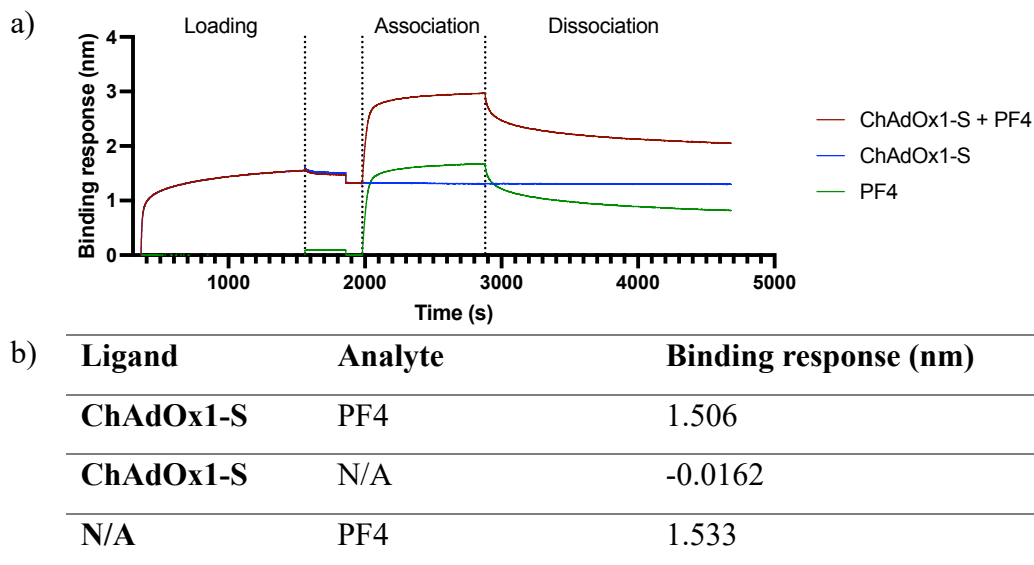


Figure 3. BLI interaction analysis of PF4 with immobilized Adv-based vaccines using amine coupling sensors. a) Sensorgram representing the binding responses of three experiments: PF4 association with sensor-immobilized ChAdOx1-S (red); assay running buffer with sensor-immobilized ChAdOx1-S (blue); and PF4 association with an empty amine coupling sensor surface (green). The loading step is shown here to illustrate that PF4 binds to the sensor regardless of whether ChAdOx1-S is loaded onto the sensor. The binding responses for each experiment are detailed in b). Immobilized ChAdOx1-S to assay running buffer is denoted as not applicable (N/A) due to the absence of analyte, and PF4 to the empty sensor surface is also denoted as N/A due to the absence of ligand. All experiments were conducted in the formulation buffer of ChAdOx1-S. Results have been normalized to the reference cell.

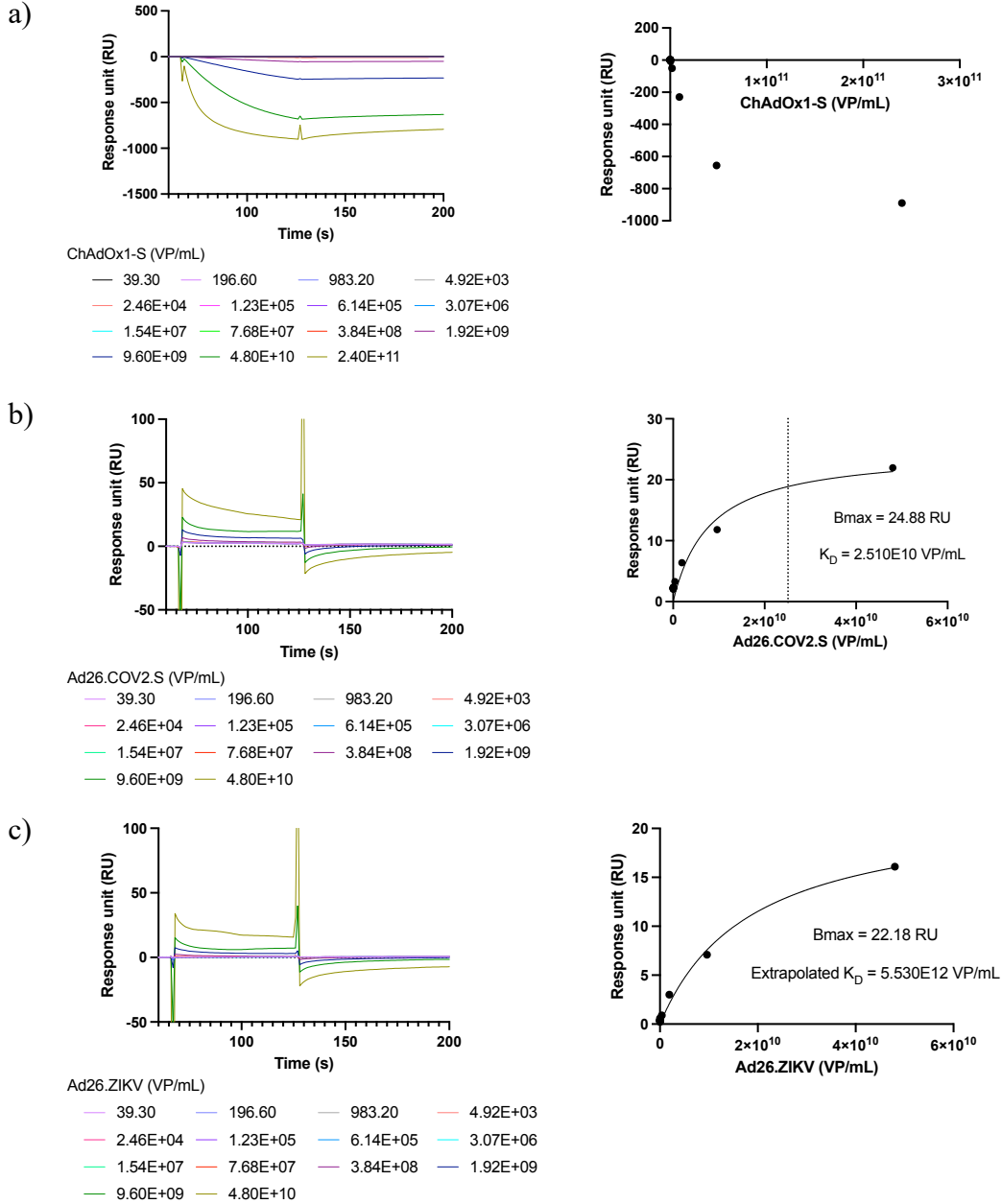


Figure 4. SPR interaction analysis of Adv-based vaccines and immobilized bPF4 using streptavidin-coated CM4 sensors. Sensorgrams representing the binding responses of bPF4 against increasing concentrations of a) ChAdOx1-S, b) Ad26.COV2.S, and c) Ad26.ZIKV. Their respective K_D and maximal binding capacity (B_{max}) were calculated using steady-state approximation based on the equilibrium binding response at each vaccine concentration. The estimated K_D for the interaction between Ad26.ZIKV and PF4 is higher than the stock concentration of Ad26.ZIKV; therefore, an extrapolated K_D is provided instead. In each experiment, approximately 500 RU of bPF4 is immobilized on a streptavidin-coated CM4 sensor chip for association with the vaccines, at a flow rate of 75 $\mu\text{L}/\text{min}$. All results have been normalized to the biotin-coated streptavidin reference flow cell.

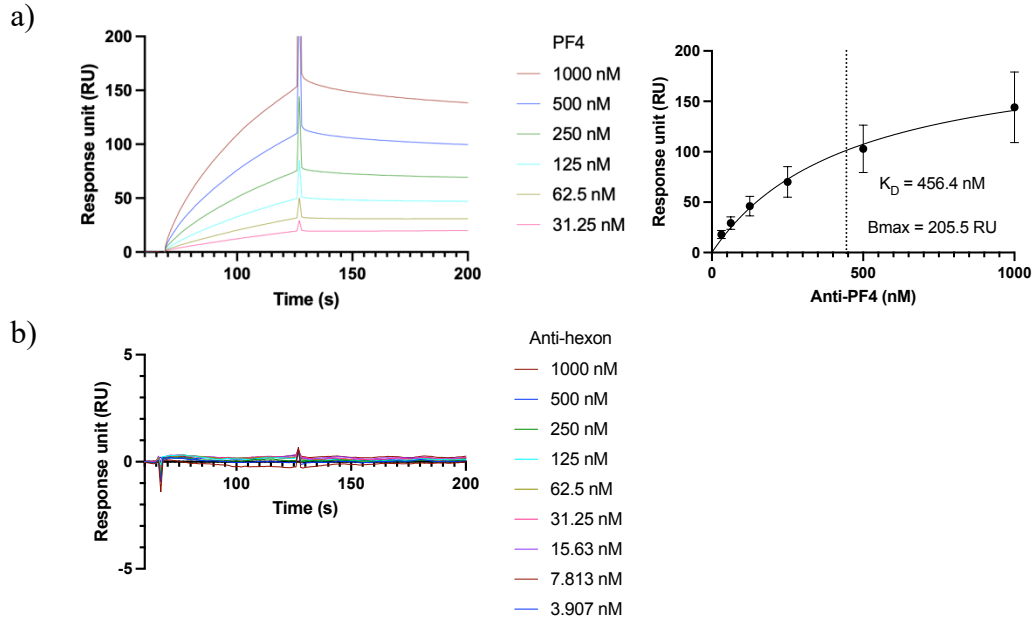


Figure 5. SPR control experiments with immobilized bPF4 using streptavidin-coated CM4 sensors. Sensorgrams representing the binding responses of bPF4 against increasing concentrations of a) the positive control polyclonal anti-PF4 and b) the negative control anti-hexon. In each experiment, approximately 500RU of bPF4 is immobilized on streptavidin-coated CM4 sensor for association with the antibodies. The K_D and B_{max} between PF4 and anti-PF4 was calculated using steady-state approximation based on the equilibrium binding response at each antibody concentration. All results have been normalized to the biotin-coated streptavidin reference flow cell.

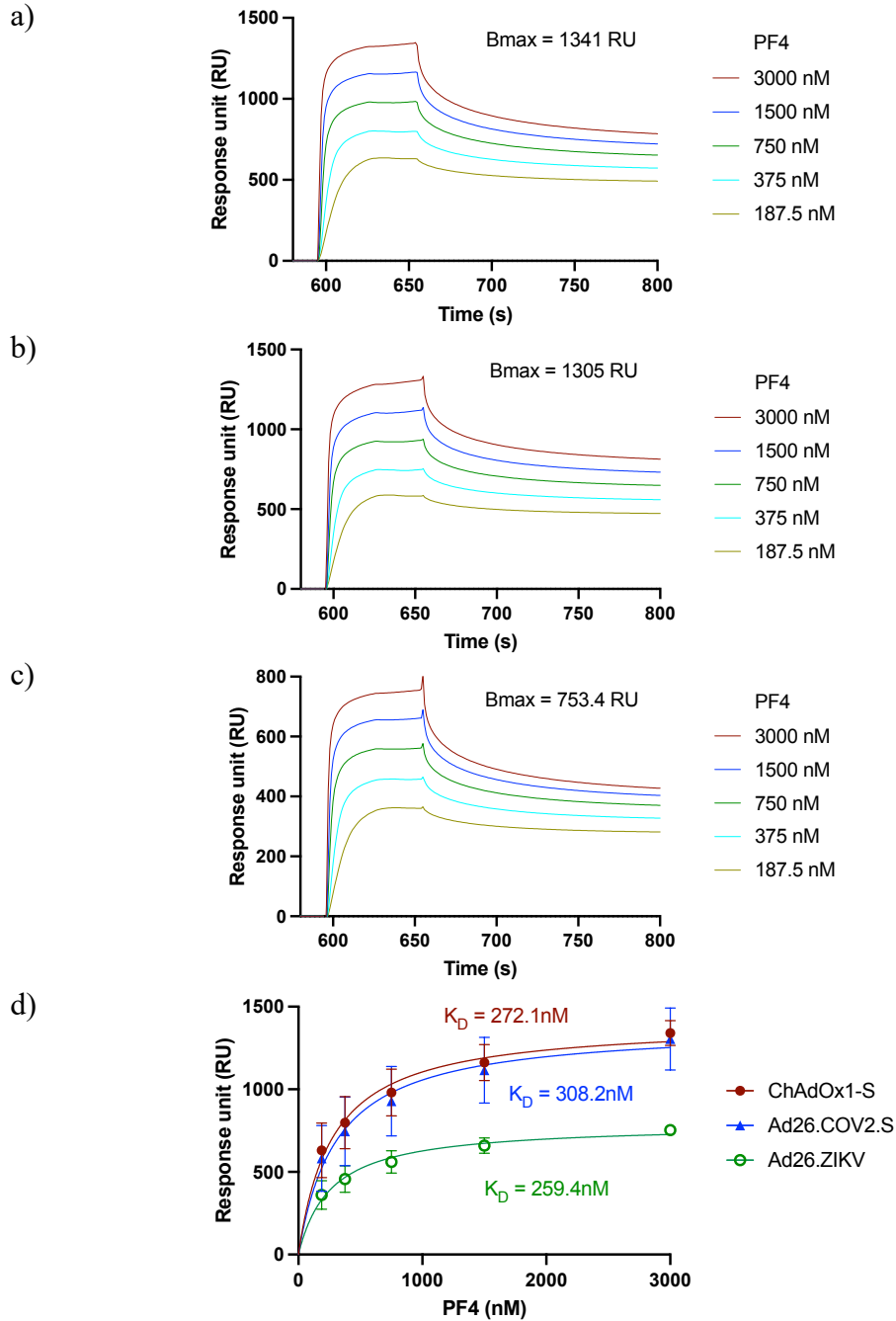


Figure 6. SPR interaction analysis of PF4 and immobilized AdV-based vaccines using anti-hexon coated amine coupling C1 sensors. Sensorgrams representing the binding responses of bPF4 against increasing concentrations of a) ChAdOx1-S, b) Ad26.COV2.S, and c) Ad26.ZIKV. Their respective K_D and B_{max} were calculated using steady-state approximation based on the equilibrium binding response at each vaccine concentration and presented in d). In each experiment, approximately 100 – 130 RU of vaccines were immobilized onto the anti-hexon coated C1 sensor for association with PF4, at a flow rate of 75 $\mu\text{L}/\text{min}$. All results have been normalized to the anti-hexon coated reference flow cell.

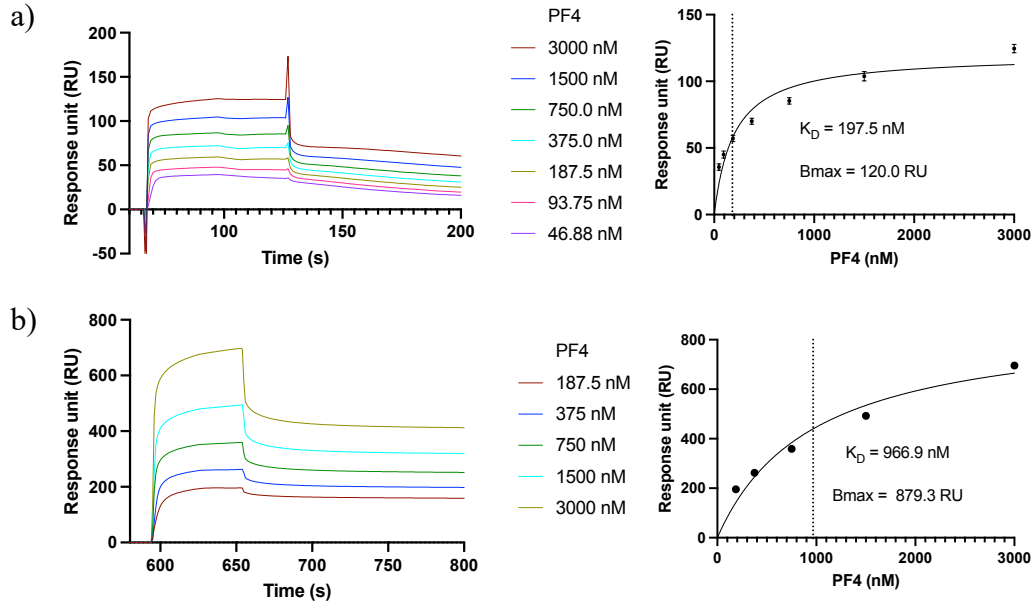


Figure 7. SPR control experiments with PF4 in the flow phase using amine coupling C1 sensors. Sensorgrams representing the binding responses of PF4 at increasing concentrations to sensor-immobilized a) positive control, polyclonal anti-PF4, and b) negative control, anti-hexon. In each experiment, approximately 500RU of control antibodies were immobilized on C1 sensor for association with PF4, at a flow rate of 75 $\mu\text{L}/\text{min}$. The K_D and B_{max} between PF4 and the antibodies were calculated using steady-state approximation based on the equilibrium binding response at each antibody concentration. All results have been normalized to a blank reference flow cell.

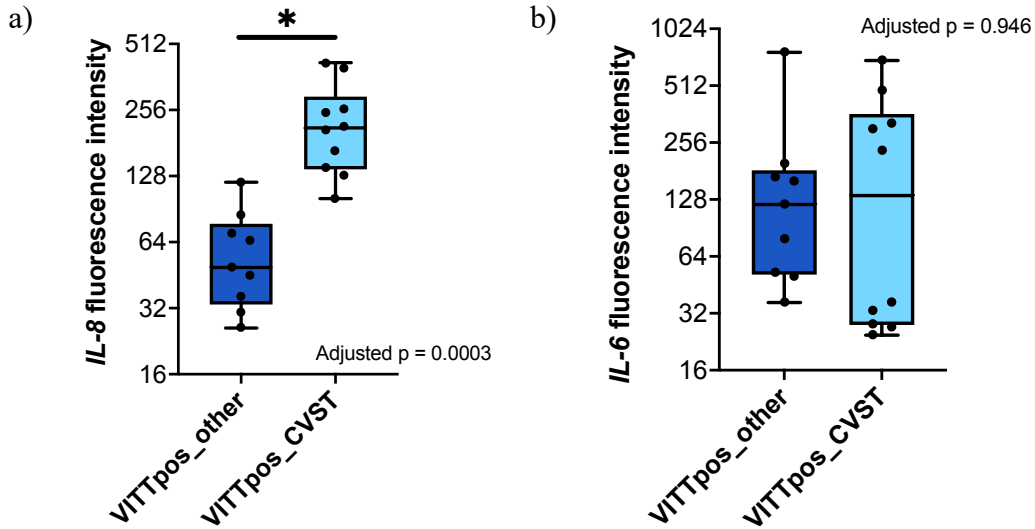


Figure 8. Cytokine level distributions in sera of VITTPos patient with and without CVST. Log2 distributions of patient sera fluorescence response for a) IL-8 and b) IL-6. The box-and-whisker plot represents the upper and lower quartiles and the median. Dark blue indicates VITTPos patients without CVST, and light blue indicates VITTPos patients with CVST. Each dot represents an individual patient. Patient sera were collected during the acute phase of their condition. Adjusted p-values were obtained from pairwise T-tests for a 48-cytokine panel, with BH adjustment. Asterisks indicate statistically significant differences between the patient cohorts (* $p < 0.05$; ** $p < 0.01$; *** $p < 0.001$).

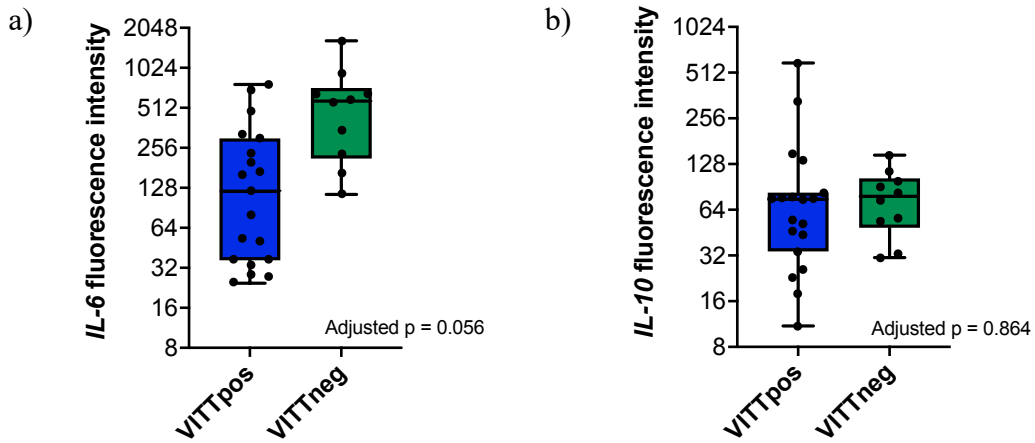


Figure 9. Cytokine level distributions of VITTPos and VITTNeg patients. Log2 distributions of patient sera fluorescence response for a) IL-6 and b) IL-10. The box-and-whisker plots represent the upper and lower quartiles and the median. Blue indicates patients diagnosed with VITT, and green indicates patients suspected of having VITT following vaccination but tested negative for anti-PF4 antibodies. Each dot represents an individual patient. Patient sera were collected during the acute phase of their condition. Adjusted p-values were obtained from pairwise T-tests for a 48-cytokine panel, with BH adjustment.

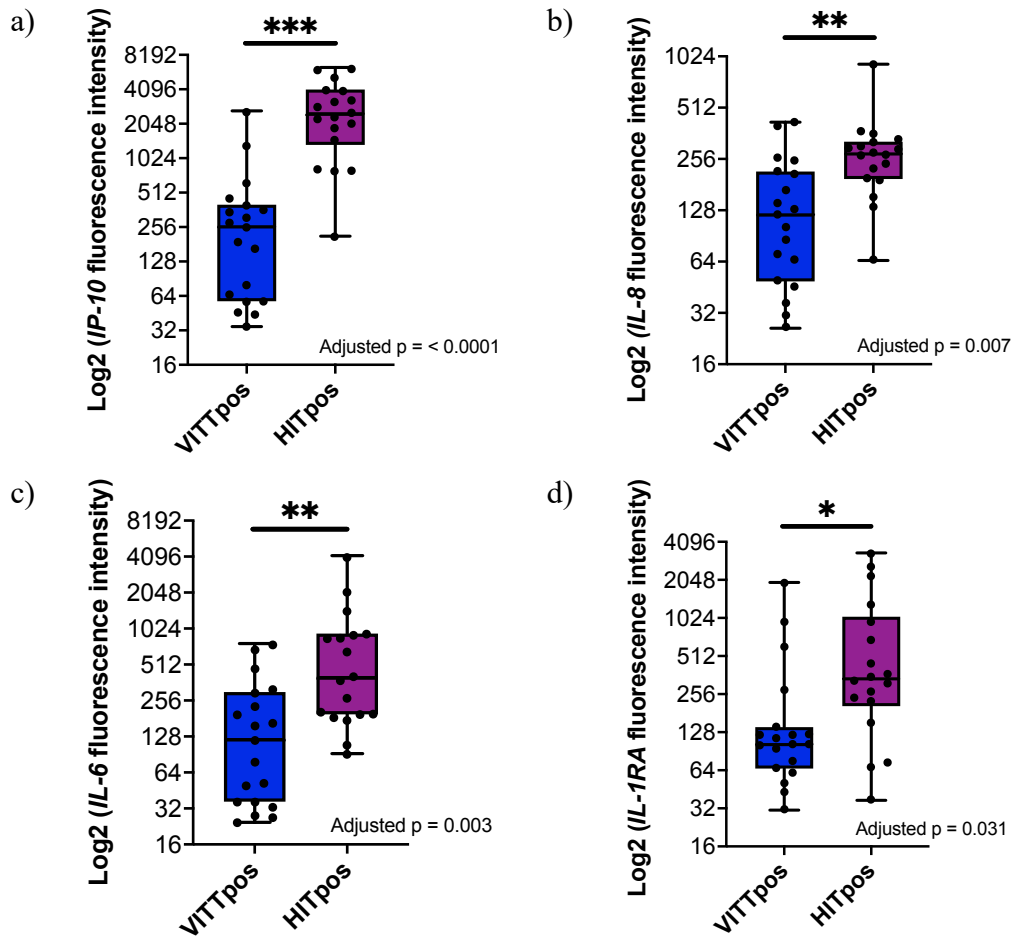


Figure 10. Cytokine level distributions of VITtpos and HITtpos patients. Distributions of patient sera fluorescence responses for a) IL-6, b) IL-8, c) IP-10, and d) IL-1RA. Each plot includes the log₂ distribution of raw data comparing cytokine levels of VITtpos to HITtpos patients. The box-and-whisker plots display the upper and lower quartiles and the median. Blue represents patients diagnosed with VITT, and purple represents the HITtpos patients. Each dot signifies an individual patient. Patient sera were collected during the acute phase of their condition. Adjusted p-values were obtained from pairwise T-tests for a 48-cytokine panel, with BH adjustment (* p < 0.05; ** p < 0.01; *** p < 0.001).

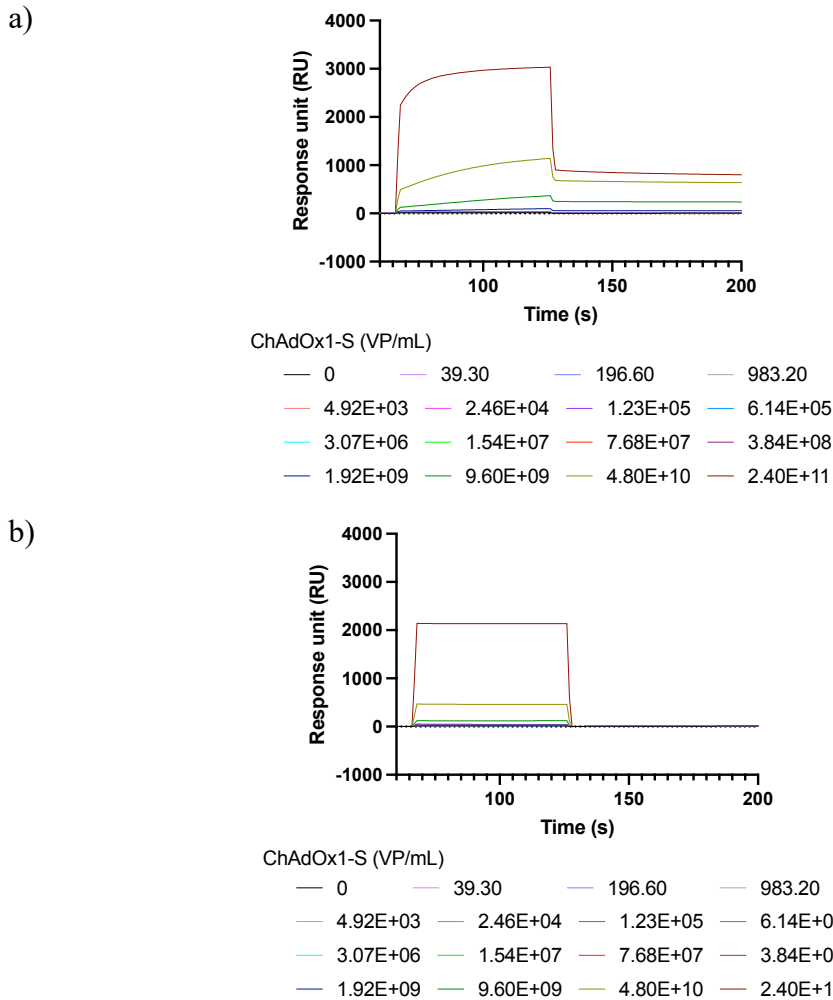
9.0 TABLES**Table 1. Cytokine profiling patient characteristics**

Characteristics	Suspected VITT		Suspected HIT
	Positive	Negative	Positive
n	19	11	19
Age (yr)	51.2 (28.4-69.2)	53.6 (40.3-68.6)	60.1 (35.0-71.8)
Sex (% male)	42.1	63.6	47.4
Arterial clot	10.5	0	
CVST (%)	52.6	9.1	
DVT (%)	15.8	31.6	
PE (%)	26.3	21.1	Not available
SVT (%)	15.8	5.3	
Platelet count (x10⁹L)	72.8 (9-301)	178.1 (60-372)	

Results expressed as means and range.

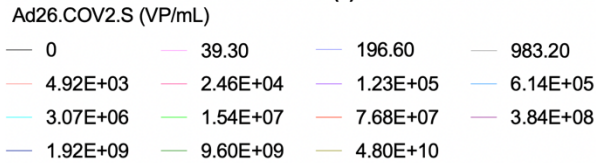
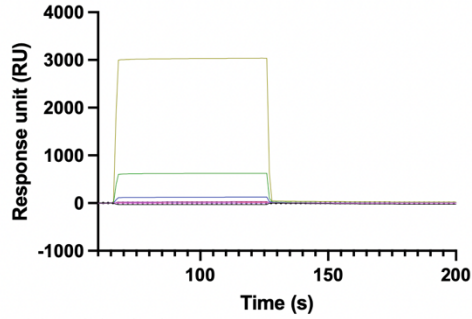
Platelet count was not available for 4 VITTPos patients.

10.0 SUPPLEMENTARY FIGURES

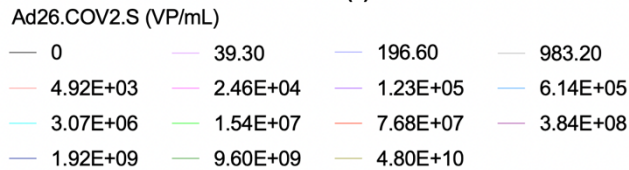
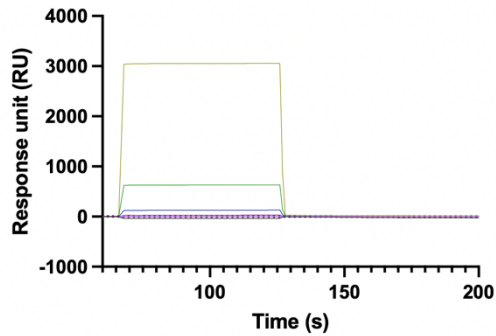


Supplementary Figure 1. Background interaction of ChAdOx1-S to streptavidin-coated reference cell using CM4 sensors in SPR. Sensorgrams representing the binding responses of ChAdOx1-S at increasing concentrations against a) a streptavidin-coated flow cell and b) a bPF4-loaded streptavidin flow cell. While a) shows the background interaction between ChAdOx1-S and the reference cell, b) presents the raw data of ChAdOx1-S binding to ~500RU of immobilized bPF4 without normalizing to the reference shown in a).

a)

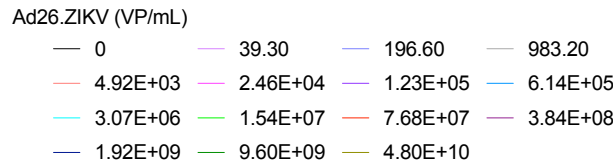
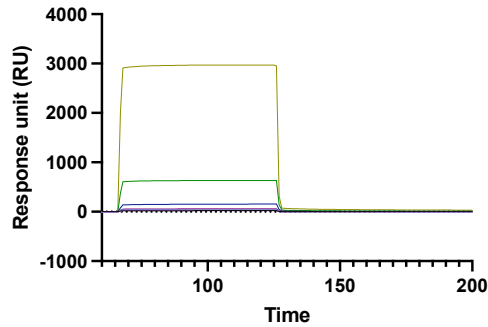


c)

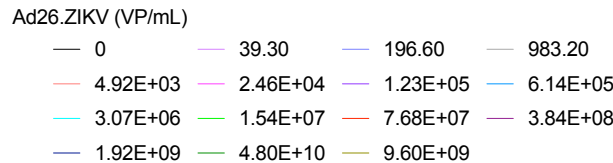
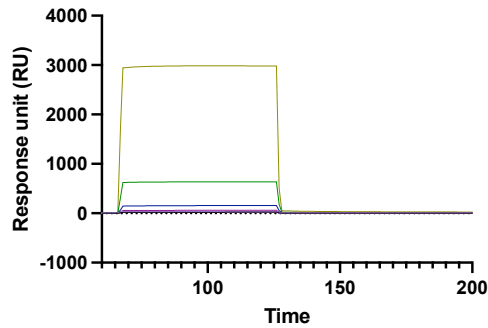


Supplementary Figure 2. Background interaction of Ad26.COV2.S to streptavidin-coated reference cell using CM4 sensors in SPR. Sensorgrams representing the binding responses of Ad26.COV2.S at increasing concentrations against a) a streptavidin-coated flow cell and b) a bPF4-loaded streptavidin flow cell. While a) shows the background interaction between Ad26.COV2.S and the reference cell, b) presents the raw data of Ad26.COV2.S binding to ~500RU of immobilized bPF4 without normalizing to the reference shown in a).

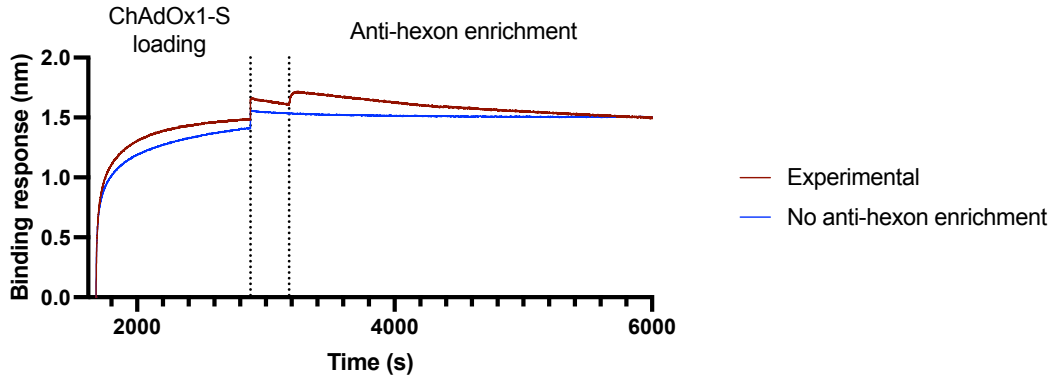
a)



c)

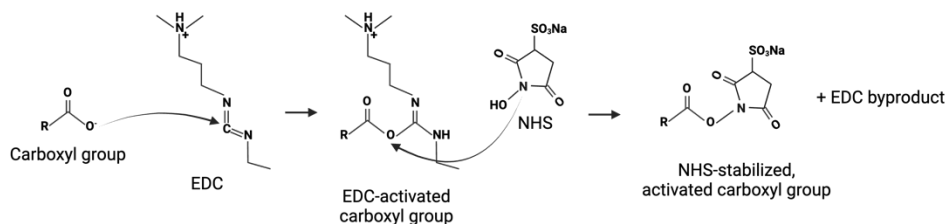


Supplementary Figure 3. Background interaction of Ad26.ZIKV to streptavidin-coated reference cell using CM4 sensors in SPR. Sensorgrams representing the binding responses of Ad26.ZIKV at increasing concentrations against a) a streptavidin-coated flow cell and b) a bPF4-loaded streptavidin flow cell. While a) shows the background interaction between Ad26.ZIKV and the reference cell, b) presents the raw data of Ad26.ZIKV binding to ~500RU of immobilized bPF4 without normalizing to the reference shown in a).

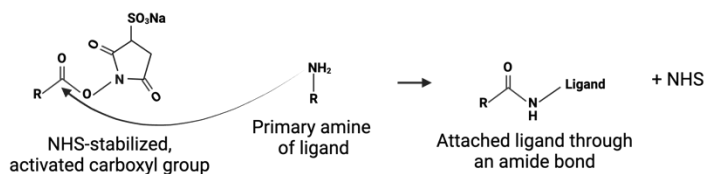


Supplementary Figure 4. BLI interaction analysis of anti-hexon detection of ChAdOx1-S captured on amine-coupled sensors. Sensorgram illustrating the binding response of 20 $\mu\text{g/mL}$ of anti-hexon associating with $1.2\text{E}12$ VP/mL of ChAdOx1-S that is captured on the sensor via immobilized anti-hexon (red); and the lack of anti-hexon detection for the sensor-captured ChAdOx1-S (blue). All experiments were conducted in the formulation buffer of ChAdOx1-S. Results have been normalized to the reference cell.

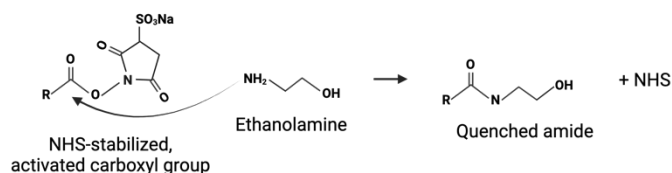
Activation



Ligand attachment



Quenching



Supplementary Figure 5. Amine coupling reaction mechanism. The chemical reaction scheme for cross-coupling a ligand containing a primary amine to the amine coupling sensor surface.¹⁴¹ The process begins with the activation of carboxyl groups by EDC and NHS, resulting in an NHS-stabilized activated carboxyl group. An electrophilic attack from the ligand primary amine establishes an amide bond between the ligand and the sensor surface. Any remaining free esters are quenched with ethanolamine, preventing further reactions with the analyte.

11.0 SUPPLEMENTARY TABLES

Cytokines (FI), median (range)	VITTpos	VITTneg	+P-value
EGF	152 (9-2932)	199.5 (9.5-1423)	0.864
Eotaxin	35.5 (13-870)	258.5 (19-1815)	0.256
FGF-2	23 (13-96)	24.5 (14-429.5)	0.420
FLT-3L	77 (24.5-285.5)	136 (56.5-351)	0.256
Fractalkine	18 (8.5-337.5)	25.5 (11.5-243.5)	0.864
G-CSF	36 (15-73.5)	59 (14-124)	0.256
GM-CSF	32 (18-434)	26 (14-60)	0.277
GROα	97 (12-452)	112.25 (17-454)	0.927
IFNα2	14 (9-83)	16 (8-355)	0.256
IFNγ	36 (22-221)	42.25 (25-632)	0.235
IL-1α	32 (14-140)	29.5 (16-135)	0.865
IL-1β	25 (17.5-194.5)	26 (13-616)	0.420
IL-1RA	102 (31-1956)	101 (34-913)	0.864
IL-2	29.5 (13-194.5)	37.5 (14-484)	0.256
IL-3	12 (9-25)	13 (10-29)	0.865
IL-4	32 (19-81.5)	46.25 (18-170)	0.256
IL-5	35 (11-189)	56 (14.5-684)	0.264
IL-6	120.5 (24.5-767.5)	575.75 (114-1636)	0.056
IL-7	44 (14.5-115)	105.5 (16.5-651.5)	0.256
IL-8	120 (26-420.5)	110 (23.5-412)	0.961
IL-9	71 (15-233)	41 (12-575)	0.865
IL-10	75 (11-592)	78.5 (31-146.5)	0.864
IL-12p40	26 (12-61)	27 (15.5-250)	0.265
IL-12p70	15 (6-32)	24.5 (12-427)	0.111
IL-13	25 (15-167.5)	27.25 (17-259)	0.408
IL-15	49 (28-84.5)	58.25 (32-338.5)	0.376
IL-17A	28.5 (12.5-132.5)	28.25 (10.5-527)	0.467
IL-17E/IL-25	27 (20-95)	39.75 (17-598.5)	0.217
IL-17F	54.5 (17-646)	49 (13-763.5)	0.754
IL-18	193 (77-345.5)	253.5 (89-552)	0.264
IL-22	59 (35-306.5)	51.25 (37-340)	0.783
IL-27	346 (17-5045)	962.25 (150-4702)	0.376
IP-10	257.5 (34.5-2656)	664.25 (71-4083)	0.235
M-CSF	102.5 (40-852)	89 (43-411)	0.864
MCP-1	2349 (33-5550.5)	3146.75 (737-9508)	0.376
MCP-3	26.5 (18.5-196.5)	31.5 (17.5-406)	0.256

MDC	9816 (2012-17404)	6907 (1001.5-10367)	0.256
MIG	1512.5 (391-8358)	2521.5 (734-17548)	0.256
MIP-1α	27 (17.5-84)	27.5 (16-341.5)	0.264
MIP-1β	751 (30-3953.5)	368.75 (151-1761)	0.449
PDGF-AA	1395 (342-8389)	2430 (147.5-7867.5)	0.783
PDGF-AB/BB	1710 (500-7593.5)	3058.5 (228-8545)	0.864
RANTES	18693.5 (258-24487)	15127 (1953-21250)	0.864
sCD40L	28.5 (15-299)	52.5 (14-739)	0.313
TGFα	100 (34-794)	73 (22-686)	0.864
TNFα	40 (18-235)	43.25 (31-304)	0.399
TNFβ	44 (28-276.5)	46 (22.5-362)	0.626
VEGF-A	375 (44-2143.5)	526.5 (42-2255)	0.467

Supplementary Table 1. Comparison of serum cytokine levels in fluorescence intensity of suspected VITT patients with and without anti-PF4 antibodies during the acute phase.

⁺ P-values for comparing cytokine levels between the VITTpos and VITTneg cohorts. Comparisons were performed using the modified T-test implemented with the *illma* package and corrected for false discovery rate due to multiple comparisons using the BH-adjustment.

Cytokines (FI), median (range)	VITPos	HITpos	[†]P-value
EGF	152 (9-2932)	40 (6-1090)	0.133
Eotaxin	35.5 (13-870)	204.5 (43-1022)	0.037*
FGF-2	23 (13-96)	32.25 (14-191)	0.766
FLT-3L	77 (24.5-285.5)	82.25 (14-755)	0.938
Fractalkine	18 (8.5-337.5)	29.75 (11.5-119)	0.999
G-CSF	36 (15-73.5)	33.5 (15-122.5)	0.935
GM-CSF	32 (18-434)	52 (13-189)	0.999
GROα	97 (12-452)	166 (25-1075)	0.353
IFNα2	14 (9-83)	17 (8-57)	0.981
IFNγ	36 (22-221)	30.5 (13-142)	0.935
IL-1α	32 (14-140)	36.5 (12.5-68)	0.835
IL-1β	25 (17.5-194.5)	32.25 (12-99)	0.999
IL-1RA	102 (31-1956)	338.25 (37-3346)	0.031*
IL-2	29.5 (13-194.5)	32 (14-133)	0.999
IL-3	12 (9-25)	10.75 (8-27)	0.834
IL-4	32 (19-81.5)	26.25 (13.5-87)	0.727
IL-5	35 (11-189)	43.5 (12-479)	0.431
IL-6	120.5 (24.5-767.5)	398.5 (92-4177)	0.003**
IL-7	44 (14.5-115)	39.75 (12-227)	0.834
IL-8	120 (26-420.5)	274 (65-921.5)	0.007**
IL-9	71 (15-233)	28 (10.5-226.5)	0.063
IL-10	75 (11-592)	137.5 (51-1795)	0.025*
IL-12p40	26 (12-61)	21.75 (12-116.5)	0.766
IL-12p70	15 (6-32)	13 (8.5-46)	0.507
IL-13	25 (15-167.5)	23 (12-63)	0.835
IL-15	49 (28-84.5)	81.25 (29-169.5)	0.031*
IL-17A	28.5 (12.5-132.5)	31.75 (7.5-154.5)	0.999
IL-17E/IL-25	27 (20-95)	34.75 (17-115)	0.834
IL-17F	54.5 (17-646)	39.75 (17-569)	0.999
IL-18	193 (77-345.5)	460.25 (144-1098)	0.0009***
IL-22	59 (35-306.5)	49.25 (26.5-107)	0.418
IL-27	346 (17-5045)	1757 (123-12294.5)	0.041*
IP-10	257.5 (34.5-2656)	2503.5 (213-6351)	6.56E-7***
M-CSF	102.5 (40-852)	92.75 (29-188)	0.315
MCP-1	2349 (33-5550.5)	3210 (801-6709)	0.688
MCP-3	26.5 (18.5-196.5)	26.25 (15-84.5)	0.948
MDC	9816 (2012-17404)	5438 (339-13447.5)	0.076

MIG	1512.5 (391-8358)	4038 (417-16298)	0.037*
MIP-1α	27 (17.5-84)	26.5 (17-86.5)	0.999
MIP-1β	751 (30-3953.5)	1255 (114-6757)	0.520
PDGF-AA	1395 (342-8389)	1207.75 (574-4232)	0.834
PDGF-AB/BB	1710 (500-7593.5)	2958.5 (423-6908)	0.727
RANTES	18693.5 (258-24487)	16082 (5910-23143)	0.999
sCD40L	28.5 (15-299)	136 (16-2212)	0.002**
TGFα	100 (34-794)	128.25 (28-396)	0.999
TNFα	40 (18-235)	80 (22.5-143)	0.063
TNFβ	44 (28-276.5)	40.5 (20-72)	0.761
VEGF-A	375 (44-2143.5)	257 (29-1893)	0.706

Supplementary Table 2. Comparison of serum cytokine levels in fluorescence intensity of VITT and HIT patients.

⁺ P-values for comparing cytokine levels between the VITTpos and HITpos cohorts. Comparisons were performed using the modified T-test implemented with the *illma* package and corrected for false discovery rate due to multiple comparisons using the BH-adjustment.

* p -value < 0.05; ** p -value < 0.01; *** p -value < 0.001.

Cytokines (FI), median (range)	VITTpos_other	VITTpos_CVST	[†]P-values
EGF	93 (9-1730)	292.5 (29-2932)	0.376
Eotaxin	83 (13-574)	34.25 (14-870)	0.978
FGF-2	21 (13.5-94)	24.25 (13-96)	0.946
FLT-3L	105 (24.5-200)	71.75 (42.5-285.5)	0.931
Fractalkine	20 (16-112)	14.5 (8.5-337.5)	0.889
G-CSF	51 (16.5-73.5)	35.5 (15-61)	0.702
GM-CSF	21 (19-61)	60 (18-434)	0.239
GROα	90 (12-302.5)	118 (18-452)	0.889
IFNα2	16 (11-51)	13 (9-83)	0.931
IFNγ	37 (24-69.5)	35 (22-221)	0.931
IL-1α	26 (14-140)	36.25 (29-83)	0.783
IL-1β	25 (17.5-194.5)	25 (17.5-69)	0.801
IL-1RA	94 (31-275.5)	121 (50-1956)	0.376
IL-2	29.5 (17-194.5)	28.75 (13-60)	0.832
IL-3	13 (11-25)	12 (9-14)	0.702
IL-4	24 (19-81.5)	33 (21-51)	0.931
IL-5	29 (22-119)	35.5 (11-189)	0.946
IL-6	120.5 (36.5-767.5)	134.25 (24.5-695.5)	0.946
IL-7	25.5 (14.5-115)	46 (17-101)	0.832
IL-8	49 (26-120)	212 (101-420.5)	0.0004***
IL-9	33 (15-233)	85.5 (21-213)	0.702
IL-10	55 (11-332)	75.5 (23-592)	0.783
IL-12p40	27 (13-61)	17.25 (12-48)	0.530
IL-12p70	15 (12-30)	16.25 (6-32)	0.931
IL-13	23 (15-53)	26 (21-167.5)	0.702
IL-15	56 (28-79)	46 (29-84.5)	0.832
IL-17A	19.5 (17-132.5)	31.5 (12.5-93)	0.946
IL-17E/IL-25	27 (22-95)	27.25 (20-43)	0.889
IL-17F	64 (17-243)	52.25 (25-646)	0.832
IL-18	178 (77-279)	195.5 (77-345.5)	0.946
IL-22	52 (35-93)	61 (44-306.5)	0.702
IL-27	263 (23.5-4229)	442.5 (17-5045)	0.889
IP-10	282.5 (44-1338)	212.25 (34.5-2656)	0.946
M-CSF	101 (42-852)	104.75 (40-502)	0.889
MCP-1	1975 (33-5550.5)	2654.75 (528-5539.5)	0.865
MCP-3	25.5 (18.5-50)	27.75 (18.5-196.5)	0.873
MDC	10476 (4548-13381)	8601 (2012-17404)	0.980

MIG	1680 (391-8358)	1495.75 (711-3569)	0.946
MIP-1α	27 (18-84)	27.5 (17.5-37)	0.832
MIP-1β	751 (30-3252)	748 (251-3953.5)	0.889
PDGF-AA	795 (342-2432)	2497 (792-8389)	0.243
PDGF-AB/BB	1308 (585-3090)	4414.25 (500-7593.5)	0.239
RANTES	17574 (258-19225)	21411.75 (8300-24487)	0.702
sCD40L	26.5 (18-299)	30.5 (15-73)	0.946
TGFα	84 (34-223)	106.25 (54-794)	0.376
TNFα	34 (23-92)	44.25 (18-235)	0.931
TNFβ	41.5 (28-47)	53.5 (30-276.5)	0.376
VEGF-A	165.5 (44-833)	578.5 (158.5-2143.5)	0.310

Supplementary Table 3. Serum cytokine levels in fluorescence intensity of VITT patients with CVST compared to those with thrombosis in other sites during the acute phase.

⁺ P-values for comparing cytokine levels between the VITTpos_{other} and VITTpos_{CVST} cohorts. Comparisons were performed using the modified T-test implemented with the *illma* package and corrected for false discovery rate due to multiple comparisons using the BH-adjustment.

* p -value < 0.05; ** p -value < 0.01; *** p -value < 0.001.

12.0 BIBLIOGRAPHY

1. Guan WJ, Ni ZY, Hu Y, et al. Clinical Characteristics of Coronavirus Disease 2019 in China. *N Engl J Med* 2020; **382**(18): 1708-20.
2. Msemburi W, Karlinsky A, Knutson V, Aleshin-Guendel S, Chatterji S, Wakefield J. The WHO estimates of excess mortality associated with the COVID-19 pandemic. *Nature* 2023; **613**(7942): 130-7.
3. Coronavirus disease (COVID-19): Herd immunity, lockdowns and COVID-19. 31 December 2020 2020. <https://www.who.int/news-room/questions-and-answers/item/herd-immunity-lockdowns-and-covid-19> (accessed 10 June 2024).
4. Krammer F. SARS-CoV-2 vaccines in development. *Nature* 2020; **586**(7830): 516-27.
5. Ndwandwe D, Wiysonge CS. COVID-19 vaccines. *Current Opinion in Immunology* 2021; **71**: 111-6.
6. How Vaccines are Developed and Approved for Use. 30 March 2023 2023. <https://www.cdc.gov/vaccines/basics/test-approve.html> (accessed 20 July 2024).
7. Chen Y, Xu Z, Wang P, et al. New-onset autoimmune phenomena post-COVID-19 vaccination. *Immunology* 2022; **165**(4): 386-401.
8. Abraham N, Spruin S, Rossi T, et al. Myocarditis and/or pericarditis risk after mRNA COVID-19 vaccination: A Canadian head to head comparison of BNT162b2 and mRNA-1273 vaccines. *Vaccine* 2022; **40**(32): 4663-71.
9. Taida T, Kato J, Ishikawa K, et al. Severe ulcerative colitis induced by COVID-19 vaccination. *Clinical Journal of Gastroenterology* 2024; **17**(3): 447-50.
10. Watanabe K, Nojima M, Nakase H, et al. Trajectory analyses to identify persistently low responders to COVID-19 vaccination in patients with inflammatory bowel disease: a prospective multicentre controlled study, J-COMBAT. *Journal of Gastroenterology* 2023; **58**(10): 1015-29.
11. Ogunjimi OB, Tsalamandris G, Paladini A, Varrassi G, Zis P. Guillain-Barré Syndrome Induced by Vaccination Against COVID-19: A Systematic Review and Meta-Analysis. *Cureus* 2023.
12. Bussel J, Cines D, Dunbar C, et al. Vaccine-induced Immune Thrombotic Thrombocytopenia. 2022. <https://www.hematology.org/covid-19/vaccine-induced-immune-thrombotic-thrombocytopenia> (accessed 7 December 2023).
13. Saluja P, Gautam N, Yadala S, Venkata AN. Thrombotic thrombocytopenic purpura (TTP) after COVID-19 vaccination: A systematic review of reported cases. *Thrombosis Research* 2022; **214**: 115-21.
14. Danish FiA, Rabani AE, Subhani FeR, Yasmin S, Koul SS. COVID-19: Vaccine-induced immune thrombotic thrombocytopenia. *European Journal of Haematology* 2022; **109**(6): 619-32.
15. Greinacher A, Thiele T, Warkentin TE, Weisser K, Kyrle PA, Eichinger S. Thrombotic Thrombocytopenia after ChAdOx1 nCov-19 Vaccination. *N Engl J Med* 2021; **384**(22): 2092-101.

16. Scully M, Singh D, Lown R, et al. Pathologic Antibodies to Platelet Factor 4 after ChAdOx1 nCoV-19 Vaccination. *N Engl J Med* 2021; **384**(23): 2202-11.
17. Schultz NH, Sorvoll IH, Michelsen AE, et al. Thrombosis and Thrombocytopenia after ChAdOx1 nCoV-19 Vaccination. *N Engl J Med* 2021; **384**(22): 2124-30.
18. Muir KL, Kallam A, Koepsell SA, Gundabolu K. Thrombotic Thrombocytopenia after Ad26.COVS Vaccination. *N Engl J Med* 2021; **384**(20): 1964-5.
19. Soboleva K, Shankar NK, Yadavalli M, et al. Geographical distribution of TTS cases following AZD1222 (ChAdOx1 nCoV-19) vaccination. *Lancet Glob Health* 2022; **10**(1): e33-e4.
20. Interim recommendations for the use of the Janssen Ad26.COVS (COVID-19) vaccine. 2022. <https://www.who.int/publications/i/item/WHO-2019-nCoV-vaccines-SAGE-recommendation-Ad26.COVS-2021.1>.
21. Stieh DJ, Barouch DH, Comeaux C, et al. Safety and Immunogenicity of Ad26-Vectored HIV Vaccine With Mosaic Immunogens and a Novel Mosaic Envelope Protein in HIV-Uninfected Adults: A Phase 1/2a Study. *J Infect Dis* 2023; **227**(8): 939-50.
22. Salisch NC, Stephenson KE, Williams K, et al. A Double-Blind, Randomized, Placebo-Controlled Phase 1 Study of Ad26.ZIKV.001, an Ad26-Vectored Anti-Zika Virus Vaccine. *Ann Intern Med* 2021; **174**(5): 585-94.
23. Kaushansky K. Thrombopoiesis. *Seminars in Hematology* 2015; **52**(1): 4-11.
24. Ghoshal K, Bhattacharyya M. Overview of Platelet Physiology: Its Hemostatic and Nonhemostatic Role in Disease Pathogenesis. *The Scientific World Journal* 2014; **2014**: 1-16.
25. Sang Y, Roest M, de Laat B, de Groot PG, Huskens D. Interplay between platelets and coagulation. *Blood Reviews* 2021; **46**.
26. Walls AC, Park YJ, Tortorici MA, Wall A, McGuire AT, Velesler D. Structure, Function, and Antigenicity of the SARS-CoV-2 Spike Glycoprotein. *Cell* 2020; **183**(6): 1735.
27. Wang S, Peng Y, Wang R, et al. Characterization of neutralizing antibody with prophylactic and therapeutic efficacy against SARS-CoV-2 in rhesus monkeys. *Nat Commun* 2020; **11**(1): 5752.
28. Folegatti PM, Ewer KJ, Aley PK, et al. Safety and immunogenicity of the ChAdOx1 nCoV-19 vaccine against SARS-CoV-2: a preliminary report of a phase 1/2, single-blind, randomised controlled trial. *The Lancet* 2020; **396**(10249): 467-78.
29. Sadoff J, Gray G, Vandebosch A, et al. Safety and Efficacy of Single-Dose Ad26.COVS Vaccine against Covid-19. *N Engl J Med* 2021; **384**(23): 2187-201.
30. Wold W, Toth K. Adenovirus Vectors for Gene Therapy, Vaccination and Cancer Gene Therapy. *Curr Gene Ther* 2013; **13**(6): 421-33.
31. Tanaka K. The proteasome: Overview of structure and functions. *Proc Jpn Acad Ser B Phys Biol Sci* 2009; **85**(1): 12-36.
32. Warkentin TE, Greinacher A. Spontaneous HIT syndrome: Knee replacement, infection, and parallels with vaccine-induced immune thrombotic thrombocytopenia. *Thromb Res* 2021; **204**: 40-51.

33. Greinacher A. Antigen generation in heparin-associated thrombocytopenia: the nonimmunologic type and the immunologic type are closely linked in their pathogenesis. *Semin Thromb Hemost* 1995; **21**(1): 106-16.
34. Nazarzadeh Zare E, Khorsandi D, Zarepour A, et al. Biomedical applications of engineered heparin-based materials. *Bioact Mater* 2024; **31**: 87-118.
35. Weitz JI. Low-molecular-weight heparins. *N Engl J Med* 1997; **337**(10): 688-98.
36. Loscalzo J, Melnick B, Handin RI. The interaction of platelet factor four and glycosaminoglycans. *Arch Biochem Biophys* 1985; **240**(1): 446-55.
37. Zucker MB, Katz IR. Platelet factor 4: production, structure, and physiologic and immunologic action. *Proc Soc Exp Biol Med* 1991; **198**(2): 693-702.
38. Arepally G, Poncz M, Cines DB. Autoantibodies in Heparin-induced thrombocytopenia. Autoantibodies. Sorrento, Campania, Italy: Elsevier Science; 2007: 511-9.
39. Cai Z, Yarovoi SV, Zhu Z, et al. Atomic description of the immune complex involved in heparin-induced thrombocytopenia. *Nat Commun* 2015; **6**: 8277.
40. Hirsh J, Warkentin TE, Shaughnessy SG, et al. Heparin and low-molecular-weight heparin: mechanisms of action, pharmacokinetics, dosing, monitoring, efficacy, and safety. *Chest* 2001; **119**(1 Suppl): 64S-94S.
41. Krauel K, Potschke C, Weber C, et al. Platelet factor 4 binds to bacteria, inducing antibodies cross-reacting with the major antigen in heparin-induced thrombocytopenia. *Blood* 2011; **117**(4): 1370-8.
42. Suh JS, Malik MI, Aster RH, Visentin GP. Characterization of the humoral immune response in heparin-induced thrombocytopenia. *Am J Hematol* 1997; **54**(3): 196-201.
43. Arepally G, McKenzie SE, Jiang XM, Poncz M, Cines DB. Fc gamma RIIA H/R 131 polymorphism, subclass-specific IgG anti-heparin/platelet factor 4 antibodies and clinical course in patients with heparin-induced thrombocytopenia and thrombosis. *Blood* 1997; **89**(2): 370-5.
44. Martel N, Lee J, Wells PS. Risk for heparin-induced thrombocytopenia with unfractionated and low-molecular-weight heparin thromboprophylaxis: a meta-analysis. *Blood* 2005; **106**(8): 2710-5.
45. Arepally GM. Heparin-induced thrombocytopenia. *Blood* 2017; **129**(21): 2864-72.
46. Bennett-Guerrero E, Slaughter TF, White WD, et al. Preoperative anti-PF4/heparin antibody level predicts adverse outcome after cardiac surgery. *The Journal of Thoracic and Cardiovascular Surgery* 2005; **130**(6): 1567-72.
47. Suh JS, Aster RH, Visentin GP. Antibodies from patients with heparin-induced thrombocytopenia/thrombosis recognize different epitopes on heparin: platelet factor 4. *Blood* 1998; **91**(3): 916-22.
48. Nazi I, Arnold DM, Warkentin TE, Smith JW, Staibano P, Kelton JG. Distinguishing between anti-platelet factor 4/heparin antibodies that can and cannot cause heparin-induced thrombocytopenia. *J Thromb Haemost* 2015; **13**(10): 1900-7.

49. Warkentin TE, Levine MN, Hirsh J, et al. Heparin-induced thrombocytopenia in patients treated with low-molecular-weight heparin or unfractionated heparin. *N Engl J Med* 1995; **332**(20): 1330-5.
50. Huynh A, Arnold DM, Kelton JG, et al. Characterization of platelet factor 4 amino acids that bind pathogenic antibodies in heparin-induced thrombocytopenia. *J Thromb Haemost* 2019; **17**(2): 389-99.
51. Arepally G, McKenzie SE, Jiang X-M, Poncz M, Cines DB. FcγRIIA H/R131 Polymorphism, Subclass-Specific IgG Anti-Heparin/Platelet Factor 4 Antibodies and Clinical Course in Patients With Heparin-Induced Thrombocytopenia and Thrombosis. *Blood* 1997; **89**(2): 370-5.
52. Ahmed I, Majeed A, Powell R. Heparin induced thrombocytopenia: diagnosis and management update. *Postgrad Med J* 2007; **83**(983): 575-82.
53. Warkentin TE. Heparin-induced thrombocytopenia-associated thrombosis: from arterial to venous to venous limb gangrene. *J Thromb Haemost* 2018; **16**(11): 2128-32.
54. Payne AB, Adamski A, Abe K, et al. Epidemiology of cerebral venous sinus thrombosis and cerebral venous sinus thrombosis with thrombocytopenia in the United States, 2018 and 2019. *Research and Practice in Thrombosis and Haemostasis* 2022; **6**(2): e12682.
55. Kehr S, Berg P, Müller S, et al. Long-term outcome of patients with vaccine-induced immune thrombotic thrombocytopenia and cerebral venous sinus thrombosis. *npj Vaccines* 2022; **7**(76).
56. Jin J, Qiao S, Liu J, et al. Neutrophil extracellular traps promote thrombogenicity in cerebral venous sinus thrombosis. *Cell & Bioscience* 2022; **12**(114).
57. Pavord S, Scully M, Hunt BJ, et al. Clinical Features of Vaccine-Induced Immune Thrombocytopenia and Thrombosis. *N Engl J Med* 2021; **385**(18): 1680-9.
58. Greinacher A, Selleng K, Warkentin TE. Autoimmune heparin-induced thrombocytopenia. *J Thromb Haemost* 2017; **15**(11): 2099-114.
59. Greinacher A, Langer F, Makris M, et al. Vaccine-induced immune thrombotic thrombocytopenia (VITT): Update on diagnosis and management considering different resources. *J Thromb Haemost* 2022; **20**(1): 149-56.
60. Bissola AL, Daka M, Arnold DM, et al. The clinical and laboratory diagnosis of vaccine-induced immune thrombotic thrombocytopenia. *Blood Adv* 2022; **6**(14): 4228-35.
61. Kanack AJ, Bayas A, George G, et al. Monoclonal and oligoclonal anti-platelet factor 4 antibodies mediate VITT. *Blood* 2022; **140**(1): 73-7.
62. Oropallo MA, Goenka R, Cancro MP. Spinal cord injury impacts B cell production, homeostasis, and activation. *Seminars in Immunology* 2014; **26**(5): 421-7.
63. Solomon GF. Stress and antibody response in rats. *Int Arch Allergy Appl Immunol* 1969; **35**(1): 97-104.
64. Rauova L, Zhai L, Kowalska MA, Arepally GM, Cines DB, Poncz M. Role of platelet surface PF4 antigenic complexes in heparin-induced thrombocytopenia pathogenesis: diagnostic and therapeutic implications. *Blood* 2006; **107**(6): 2346-53.

65. Huynh A, Kelton JG, Arnold DM, Daka M, Nazy I. Antibody epitopes in vaccine-induced immune thrombotic thrombocytopenia. *Nature* 2021; **596**(7873): 565-9.
66. Baker AT, Mundy RM, Davies JA, Rizkallah PJ, Parker AL. Human adenovirus type 26 uses sialic acid-bearing glycans as a primary cell entry receptor. *Sci Adv* 2019; **5**(9): eaax3567.
67. Greinacher A, Selleng K, Palankar R, et al. Insights in ChAdOx1 nCoV-19 vaccine-induced immune thrombotic thrombocytopenia. *Blood* 2021; **138**(22): 2256-68.
68. Baker AT, Boyd RJ, Sarkar D, et al. ChAdOx1 interacts with CAR and PF4 with implications for thrombosis with thrombocytopenia syndrome. *Sci Adv* 2021; **7**(49): eabl8213.
69. Michalik S, Siegerist F, Palankar R, et al. Comparative analysis of ChAdOx1 nCoV-19 and Ad26.COV2.S SARS-CoV-2 vector vaccines. *Haematologica* 2022; **107**(4): 947-57.
70. Krutzke L, Rosler R, Allmendinger E, Engler T, Wiese S, Kochanek S. Process- and product-related impurities in the ChAdOx1 nCov-19 vaccine. *Elife* 2022; **11**.
71. Eichinger S, Warkentin TE, Greinacher A. Thrombotic Thrombocytopenia after ChAdOx1 nCoV-19 Vaccination. Reply. *N Engl J Med* 2021; **385**(3): e11.
72. Kany S, Vollrath JT, Relja B. Cytokines in Inflammatory Disease. *Int J Mol Sci* 2019; **20**(23).
73. Chen L, Deng H, Cui H, et al. Inflammatory responses and inflammation-associated diseases in organs. *Oncotarget* 2018; **9**(6): 7204-18.
74. Najem MY, Couturand F, Lemarié CA. Cytokine and chemokine regulation of venous thromboembolism. *Journal of Thrombosis and Haemostasis* 2020; **18**(5): 1009-19.
75. van Aken B, Reitsma P, Rosendaal F. Interleukin 8 and venous thrombosis: evidence for a role of inflammation in thrombosis. *British Journal of Haematology* 2002; **116**(1): 173-7.
76. Aloui C, Prigent A, Sut C, et al. The signaling role of CD40 ligand in platelet biology and in platelet component transfusion. *Int J Mol Sci* 2014; **15**(12): 22342-64.
77. de Buhr N, Baumann T, Werlein C, et al. Insights Into Immunothrombotic Mechanisms in Acute Stroke due to Vaccine-Induced Immune Thrombotic Thrombocytopenia. *Frontiers in Immunology* 2022; **13**.
78. Nazy I, Clare R, Staibano P, et al. Cellular immune responses to platelet factor 4 and heparin complexes in patients with heparin-induced thrombocytopenia. *Journal of Thrombosis and Haemostasis* 2018; **16**(7): 1402-12.
79. Shi C, Wang C, Wang H, et al. The Potential of Low Molecular Weight Heparin to Mitigate Cytokine Storm in Severe COVID-19 Patients: A Retrospective Cohort Study. *Clin Transl Sci* 2020; **13**(6): 1087-95.
80. Litov L, Petkov P, Rangelov M, et al. Molecular Mechanism of the Anti-Inflammatory Action of Heparin. *International Journal of Molecular Sciences* 2021; **22**(19).

81. Hasan M, Najjam S, Gordon MY, Gibbs RV, Rider CC. IL-12 Is a Heparin-Binding Cytokine. *The Journal of Immunology* 1999; **162**(2): 1064-70.
82. Collignon C, Bol V, Chalon A, et al. Innate Immune Responses to Chimpanzee Adenovirus Vector 155 Vaccination in Mice and Monkeys. *Frontiers in Immunology* 2020; **11**.
83. Teigler JE, Iampietro MJ, Barouch DH. Vaccination with Adenovirus Serotypes 35, 26, and 48 Elicits Higher Levels of Innate Cytokine Responses than Adenovirus Serotype 5 in Rhesus Monkeys. *Journal of Virology* 2012; **86**(18): 9590-8.
84. Moens L, Tangye SG. Cytokine-Mediated Regulation of Plasma Cell Generation: IL-21 Takes Center Stage. *Frontiers in Immunology* 2014; **5**.
85. Granato A, Hayashi EA, Baptista BJA, Bellio M, Nobrega A. IL-4 Regulates Bim Expression and Promotes B Cell Maturation in Synergy with BAFF Conferring Resistance to Cell Death at Negative Selection Checkpoints. *The Journal of Immunology* 2014; **192**(12): 5761-75.
86. Strengell M, Sareneva T, Foster D, Julkunen I, Matikainen S. IL-21 Up-Regulates the Expression of Genes Associated with Innate Immunity and Th1 Response. *The Journal of Immunology* 2002; **169**(7): 3600-5.
87. Dienz O, Eaton SM, Bond JP, et al. The induction of antibody production by IL-6 is indirectly mediated by IL-21 produced by CD4⁺ T cells. *Journal of Experimental Medicine* 2009; **206**(1): 69-78.
88. Vos Q, Lees A, Wu Z, Snapper CM, Mond JJ. B-cell activation by T-cell-independent type 2 antigens as an integral part of the humoral immune response to pathogenic microorganisms. *Immunological Reviews* 2000; **176**(1): 154-70.
89. Peçanha LM, Snapper CM, Lees A, Mond JJ. Lymphokine control of type 2 antigen response. IL-10 inhibits IL-5- but not IL-2-induced Ig secretion by T cell-independent antigens. *The Journal of Immunology* 1992; **148**(11): 3427-32.
90. Kim M, Kim T-J, Kim HM, Doh J, Lee K-M. Multi-cellular natural killer (NK) cell clusters enhance NK cell activation through localizing IL-2 within the cluster. *Scientific Reports* 2017; **7**(1).
91. van der Neut Kolfschoten M, Inganäs H, Perez-Peinado C, et al. Biophysical studies do not reveal direct interactions between human PF4 and Ad26.COV2.S vaccine. *Journal of Thrombosis and Haemostasis* 2024; **22**(4): 1046-55.
92. Murali S, Rustandi RR, Zheng X, Payne A, Shang L. Applications of Surface Plasmon Resonance and Biolayer Interferometry for Virus-Ligand Binding. *Viruses* 2022; **14**(4).
93. van der Merwe P. Surface Plasmon Resonance. Protein-Ligand Interactions: hydrodynamic and calorimetry. USA: Oxford University Press; 2001: 137–70.
94. Soltermann F, Struwe WB, Kukura P. Label-free methods for optical in vitro characterization of protein-protein interactions. *Phys Chem Chem Phys* 2021; **23**(31): 16488-500.
95. Kamat V, Rafique A. Designing binding kinetic assay on the bio-layer interferometry (BLI) biosensor to characterize antibody-antigen interactions. *Analytical Biochemistry* 2017; **536**: 16-31.

96. Yang D, Singh A, Wu H, Kroe-Barrett R. Comparison of biosensor platforms in the evaluation of high affinity antibody-antigen binding kinetics. *Analytical Biochemistry* 2016; **508**: 78-96.
97. Custers J, Kim D, Leyssen M, et al. Vaccines based on replication incompetent Ad26 viral vectors: Standardized template with key considerations for a risk/benefit assessment. *Vaccine* 2021; **39**(22): 3081-101.
98. Breen EJ, Tan W, Khan A. The Statistical Value of Raw Fluorescence Signal in Luminex xMAP Based Multiplex Immunoassays. *Sci Rep* 2016; **6**: 26996.
99. Ritchie ME, Phipson B, Wu D, et al. limma powers differential expression analyses for RNA-sequencing and microarray studies. *Nucleic Acids Res* 2015; **43**(7): e47.
100. Benjamini Y, Hochberg Y. Controlling the False Discovery Rate: A Practical and Powerful Approach to Multiple Testing. *Journal of the Royal Statistical Society* 1995; **57**(1): 289-300.
101. Light DW, Lexchin J. The costs of coronavirus vaccines and their pricing. *Journal of the Royal Society of Medicine* 2021; **114**(11): 502-4.
102. Zhang X, Chen L, Bancroft D. Crystal structure of human recombinant platelet factor 4. *Biochemistry* 1994; **33**: 8361-6.
103. Marn AM, Needham J, Chiodi E, Unlu MS. Multiplexed, High-Sensitivity Measurements of Antibody Affinity Using Interferometric Reflectance Imaging Sensor. *Biosensors (Basel)* 2021; **11**(12).
104. Kajon A, Lynch J. Adenovirus: Epidemiology, Global Spread of Novel Serotypes, and Advances in Treatment and Prevention. *Seminars in Respiratory and Critical Care Medicine* 2016; **37**(04): 586-602.
105. Robinson CM, Singh G, Lee JY, et al. Molecular evolution of human adenoviruses. *Sci Rep* 2013; **3**: 1812.
106. Bradley RR, Maxfield LF, Lynch DM, Iampietro MJ, Borducchi EN, Barouch DH. Adenovirus serotype 5-specific neutralizing antibodies target multiple hexon hypervariable regions. *J Virol* 2012; **86**(2): 1267-72.
107. Markotter W, Walsh MP, Chintakuntlawar A, et al. Evidence of Molecular Evolution Driven by Recombination Events Influencing Tropism in a Novel Human Adenovirus that Causes Epidemic Keratoconjunctivitis. *PLoS ONE* 2009; **4**(6).
108. Tanaka T, Narazaki M, Kishimoto T. IL-6 in inflammation, immunity, and disease. *Cold Spring Harb Perspect Biol* 2014; **6**(10): a016295.
109. Yao G, Ma C, Liu J, Sun Z, Wei B. Interleukin-6 serum levels are independently associated with severe adenovirus pneumonia in children: a cross-sectional study. *Transl Pediatr* 2022; **11**(12): 1962-71.
110. Bosseboeuf A, Allain-Maillet S, Mennesson N, et al. Pro-inflammatory State in Monoclonal Gammopathy of Undetermined Significance and in Multiple Myeloma Is Characterized by Low Sialylation of Pathogen-Specific and Other Monoclonal Immunoglobulins. *Frontiers in Immunology* 2017; **8**.
111. Ferman J, Bridoux F, Dispenzieri A, et al. Monoclonal gammopathy of clinical significance: a novel concept with therapeutic implications. *Blood* 2018; **132**(14): 1478–85.

112. Gkalea V, Fotiou D, Dimopoulos MA, Kastritis E. Monoclonal Gammopathy of Thrombotic Significance. *Cancers* 2023; **15**(2).
113. Kristinsson SY, Pfeiffer RM, Björkholm M, et al. Arterial and venous thrombosis in monoclonal gammopathy of undetermined significance and multiple myeloma: a population-based study. *Blood* 2010; **115**(24): 4991-8.
114. Gkalea V, Fotiou D, Dimopoulos MA, Kastritis E. Monoclonal Gammopathy of Thrombotic Significance. *Cancers (Basel)* 2023; **15**(2).
115. Kanack AJ, Schaefer JK, Sridharan M, et al. Monoclonal gammopathy of thrombotic/thrombocytopenic significance. *Blood* 2023; **141**(14): 1772-6.
116. Greinacher A, Langer F, Schonborn L, et al. Platelet-activating anti-PF4 antibodies mimic VITT antibodies in an unvaccinated patient with monoclonal gammopathy. *Haematologica* 2022; **107**(5): 1219-21.
117. Muslimani AA, Spiro TP, Chaudhry AA, Taylor HC, Jaiyesimi I, Daw HA. Venous thromboembolism in patients with monoclonal gammopathy of undetermined significance. *Clin Adv Hematol Oncol* 2009; **7**(12): 827-32.
118. Iyer S, Cheng G. Role of Interleukin 10 Transcriptional Regulation in Inflammation and Autoimmune Disease. *Crit Rev Immunol* 2012; **32**(1): 23–63.
119. Yi Z, Ma T, Liu J, et al. The yin–yang effects of immunity: From monoclonal gammopathy of undetermined significance to multiple myeloma. *Frontiers in Immunology* 2022; **13**.
120. Pouplard C, Cornillet-Lefebvre P, Attaoua R, et al. Interleukin-10 promoter microsatellite polymorphisms influence the immune response to heparin and the risk of heparin-induced thrombocytopenia. *Thromb Res* 2012; **129**(4): 465-9.
121. Alexandrakis MG, Goulidaki N, Pappa CA, et al. Interleukin-10 Induces Both Plasma Cell Proliferation and Angiogenesis in Multiple Myeloma. *Pathology & Oncology Research* 2015; **21**(4): 929-34.
122. Warkentin TE. Platelet-activating anti-PF4 disorders: An overview. *Semin Hematol* 2022; **59**(2): 59-71.
123. Harker JA, Greene TT, Barnett BE, Bao P, Dolgoter A, Zuniga EI. IL-6 and IL-27 play both distinct and redundant roles in regulating CD4 T-cell responses during chronic viral infection. *Front Immunol* 2023; **14**: 1221562.
124. Arend W, Malyak M, Guthridge C, Gabay C. Interleukin-1 Receptor Antagonist: Role in Biology. *Annu Rev Immunol* 1998; **16**: 27-55.
125. Friberg D, Bryant J, Shannon W, Whiteside T. In Vitro Cytokine Production by Normal Human Peripheral Blood Mononuclear Cells as a Measure of Immunocompetence or the State of Activation. *Clin Diagn Lab Immunol* 1994; **1**(3): 261-8.
126. Ashraf SS, Tian Y, Zacharias S, Cowan D, Martin P, Watterson K. Effects of cardiopulmonary bypass on neonatal and paediatric inflammatory profiles. *Eur J Cardiothorac Surg* 1997; **12**(6): 862-8.
127. Alcaraz AJ, Manzano L, Sancho L, et al. Different proinflammatory cytokine serum pattern in neonate patients undergoing open heart surgery. Relevance of IL-8. *J Clin Immunol* 2005; **25**(3): 238-45.
128. Prince N, Penatzer JA, Dietz MJ, Boyd JW. Localized cytokine responses to total knee arthroplasty and total knee revision complications. *J Transl Med* 2020; **18**(1): 330.

129. Mukaida N, Harada A, Matsushima K. Interleukin-8 (IL-8) and monocyte chemotactic and activating factor (MCAF/MCP-1), chemokines essentially involved in inflammatory and immune reactions. *Cytokine Growth Factor Rev* 1998; **9**(1): 9-23.
130. Mutua V, Gershwin LJ. A Review of Neutrophil Extracellular Traps (NETs) in Disease: Potential Anti-NETs Therapeutics. *Clinical Reviews in Allergy & Immunology* 2021; **61**(2): 194-211.
131. Leung HHL, Perdomo J, Ahmadi Z, et al. NETosis and thrombosis in vaccine-induced immune thrombotic thrombocytopenia. *Nat Commun* 2022; **13**(1): 5206.
132. Holm S, Kared H, Michelsen AE, et al. Immune complexes, innate immunity, and NETosis in ChAdOx1 vaccine-induced thrombocytopenia. *Eur Heart J* 2021; **42**(39): 4064-72.
133. Gollomp K, Kim M, Johnston I, et al. Neutrophil accumulation and NET release contribute to thrombosis in HIT. *JCI Insight* 2018; **3**(18): e99445.
134. Perdomo J, Leung HHL, Ahmadi Z, et al. Neutrophil activation and NETosis are the major drivers of thrombosis in heparin-induced thrombocytopenia. *Nature Communications* 2019; **10**(1322).
135. Carnevale R, Leopizzi M, Dominici M, et al. PAD4-Induced NETosis Via Cathepsin G-Mediated Platelet-Neutrophil Interaction in ChAdOx1 Vaccine-Induced Thrombosis-Brief Report. *Arterioscler Thromb Vasc Biol* 2023; **43**(10): e396-e403.
136. Atta-ur-Rahman, Harvey K, Siddiqui R. Interleukin-8: An autocrine inflammatory mediator. *Curr Pharm Des* 1999; **5**(4).
137. Huynh A, Arnold DM, Ivetic N, et al. Antibodies against platelet factor 4 and the risk of cerebral venous sinus thrombosis in patients with vaccine-induced immune thrombotic thrombocytopenia. *Journal of Thrombosis and Haemostasis* 2023.
138. Nery F, Carneiro P, Correia S, et al. Systemic inflammation as a risk factor for portal vein thrombosis in cirrhosis: a prospective longitudinal study. *European Journal of Gastroenterology & Hepatology* 2020; **33**(1S): e108-e13.
139. Ding J, Pan L, Lan D, et al. Inflammatory Markers Differentiate Cerebral Venous Sinus Thrombosis from Mimics. *Thrombosis and Haemostasis* 2022; **123**(03): 326-35.
140. Dutta A, Ghosh R, Bhattacharya D, et al. Anti-PF4 antibody negative cerebral venous sinus thrombosis without thrombocytopenia following immunization with COVID-19 vaccine in an elderly non-comorbid Indian male, managed with conventional heparin-warfarin based anticoagulation. *Diabetes & Metabolic Syndrome: Clinical Research & Reviews* 2021; **15**(4).
141. Fischer M. Amine Coupling Through EDC/NHS: A Practical Approach. *Surface Plasmon Resonance*: Humana Press; 2010: 55-73.